

We thank the reviewer for the constructive criticism and helpful comments. Our replies to the individual points are given below.

1. The explanation for the derivation of tau_PBL (p. 18, l. 7-24) is still unclear. First, isn't this actually an estimate of the boundary layer residence time, and not a PBL "mixing time" as stated in the text? Second, I think it is not surprising that the PBL mixing time is far shorter than the overall residence time, and I don't think this needs such a detailed explanation. But, it is still not clear in the revised text how this particular value was arrived at. This is rather important since the emissions are determined by linear regression of Eq. (7) against the concentrations. Choosing a different value for tau will result in a different overall scaling of the emission equation as given in Eq. 8, correct?

I have the impression that tau was arrived at by tuning the overall emissions up or down until the concentrations approximately matched the concentrations produced by the model. Given the amount of uncertainty in this problem, this is probably a "good enough" optimization procedure, but please clarify whether this is the case and explain clearly in the text.

The reviewer is correct in all points. The text in the manuscript has been reformulated as follows:

“In eq. (7), the FBAP lifetime τ represents a boundary layer residence time. For an initial test simulation, τ was assumed to be constant and estimated with an initial value of one day, as given in literature for atmospheric lifetimes of aerosol particles with 3 μm in diameter (Jaenicke, 1978). In this test simulation, the resulting FBAP concentrations were about a factor of 5 lower compared to the FBAP measurements. As a remedy, τ is heuristically adjusted to $\tau = 4 \frac{3}{4}$ hours, such that the simulated concentrations on average match the observed concentrations. The deviation from a lifetime of 3 μm particles given in literature may be attributed to different factors, like the vertical variation of the concentration of fungal spores within the boundary layer (example shown in Figure 7), the broad size distribution of FBAP particles (see Figure 1), advection processes, non-equilibrium conditions, and the exchange with the free troposphere and the much longer lifetime of spores above the boundary layer.”

2. p. 15, l. 29-30: "These competing effects are impossible to separate when only point measurements are available." I disagree with this statement, although I would agree that it is likely that more measurements and/or further analysis (for instance, further model sensitivity tests) would be needed. With enough measurements and careful analysis, it should be possible to tease apart some of these effects. (measurements of vertical profiles, and accompanying measurements of meteorological variables, would be helpful, too)

We agree with the reviewer that with the help of auxiliary measurements, more information on potential FBAP sources and methods like positive matrix factorization, the different impacts on FBAP concentrations could be further disentangled. However, we believe that our present dataset does not offer that possibility.

In the text, “impossible” has been replaced by “difficult”.

3. Incidentally, I disagree strongly with the previous reviewer's implication that "simply eliminat[ing] bias" does not constitute an improvement in model skill. Bias is generally considered to be an important component of model skill (e.g., Murphy and Epstein, 1989), and reducing bias is valuable and important!

We would like to thank the reviewer for his/her encouraging comment.

1 **Regional-scale Simulations of Fungal Spore Aerosols**
2 **Using an Emission Parameterization Adapted to Local**
3 **Measurements of Fluorescent Biological Aerosol Particles**

4
5
6 **M. Hummel^{1,*}, C. Hoose¹, M. Gallagher², D. A. Healy³, J. A. Huffman⁴,**
7 **D. O'Connor³, U. Pöschl⁵, C. Pöhlker⁵, N. H. Robinson⁶, M. Schnaiter¹,**
8 **J. R. Sodeau³, M. Stengel⁷, E. Toprak¹, and H. Vogel¹**

9 [1]{Institute for Meteorology and Climate Research, Karlsruhe Institute of Technology,
10 Karlsruhe, Germany}

11 [2]{The Centre for Atmospheric Sciences, The University of Manchester, Manchester, UK}

12 [3]{Centre for Research into Atmospheric Chemistry, Department of Chemistry, University
13 College Cork, Cork, Ireland}

14 [4]{Department of Chemistry & Biochemistry, University of Denver, Denver, Colorado,
15 USA}

16 [5]{Biogeochemistry Department and Multiphase Chemistry Department, Max Planck
17 Institute for Chemistry, Mainz, Germany}

18 [6]{Met Office, Exeter, UK}

19 [7]{Deutscher Wetterdienst (DWD), Offenbach, Germany}

20 [*]{now at: Department of Geosciences, University of Oslo, Norway}

21 Correspondence to: M. Hummel (matthias.hummel@kit.edu) and C. Hoose
22 (corinna.hoose@kit.edu)

23
24 **Abstract**

25 Fungal spores as a prominent type of primary biological aerosol particles (PBAP) have been
26 incorporated into the COSMO-ART regional atmospheric model. Two literature-based
27 emission rates for fungal spores derived from fungal spore colony counts and chemical tracer

1 measurements were used as a parameterization baseline for this study. A third, new emission
2 parameterization for fluorescent biological aerosol particles (FBAP) was adapted to field
3 measurements from four locations across Europe. FBAP concentrations can be regarded as a
4 lower estimate of total PBAP concentrations. Size distributions of FBAP often show a distinct
5 mode at approx. 3 μm , corresponding to a diameter range characteristic for many fungal
6 spores. Previous studies for several locations have suggested that FBAP are in many cases
7 dominated by fungal spores. Thus, we suggest that simulated FBAP and fungal spore
8 concentrations obtained from the three different emission parameterizations can be compared
9 to FBAP measurements. The comparison reveals that simulated fungal spore concentrations
10 based on literature emission parameterizations are lower than measured FBAP concentrations.
11 In agreement with the measurements, the model results show a diurnal cycle in simulated
12 fungal spore concentrations, which may develop partially as a consequence of a varying
13 boundary layer height between day and night. Temperature and specific humidity, together
14 with leaf area index, were chosen to drive the new emission parameterization which is fitted
15 to the FBAP observations. The new parameterization results in similar root mean square
16 errors and correlation coefficients compared to the FBAP observations as the previously
17 existing fungal spore emission parameterizations, with some improvements in the bias. Using
18 the new emission parameterization on a model domain covering Western Europe, FBAP in
19 the lowest model layer comprise a fraction of 15% of the total aerosol mass over land and
20 reach average number concentrations of 26 L^{-1} . The results confirm that fungal spores and
21 biological particles may account for a major fraction of supermicron aerosol particle number
22 and mass concentration over vegetated continental regions and should thus be explicitly
23 considered in air quality and climate studies.

24

25 **1. Introduction**

26 Particles emitted from biological sources are a miscellaneous and omnipresent group of the
27 Earth's atmospheric aerosols (Elbert et al., 2007; Després et al., 2012). These primary
28 biological aerosol particles (PBAP) can be transported over large distances and their impacts
29 are studied by various fields of research, such as atmospheric science, agricultural research,
30 biogeography and public health (Burrows et al., 2009). PBAP are solid airborne particles of
31 biological origin and include microorganisms or reproductive units (e.g. bacteria, fungi,
32 spores, pollen or viruses) as well as excretions and fragments of biological organisms (e.g.

1 detritus, microbial fragments or leaf debris) (Després et al., 2012). Typical sizes range from
2 $< 0.3 \mu\text{m}$ for viruses to diameters of single bacteria ($0.25 - 3 \mu\text{m}$), bacteria agglomerates
3 ($3 - 8 \mu\text{m}$), fungal spores ($1 - 30 \mu\text{m}$), and up to $10 - 100 \mu\text{m}$ for airborne pollen (Jones and
4 Harrison, 2004; Shaffer and Lighthart, 1997; Després et al., 2012).

5 The share of atmospheric aerosol composition belonging to PBAP is large and possibly
6 underestimated (Jaenicke et al., 2007), but is also very uncertain. Estimates of relative PBAP
7 fraction from global models and local measurements reveal large differences between reports.
8 On one hand, the calculated number concentration of PBAP (zonal annual mean surface
9 concentrations of $10^{-2} - 10^{-1} \text{cm}^{-3}$) is less than that of mineral dust (65cm^{-3}) or soot
10 (1000cm^{-3}) concentrations by several orders of magnitude (Hoose et al., 2010b). Modeling
11 studies have yielded global source strengths of $\sim 10 \text{Tg/yr}$ (plant debris and fungal spores,
12 Winiwarter et al., 2009), 56Tg/yr (all PBAP types, Penner, 1995), 78Tg/yr (bacteria, fungal
13 spores and pollen, Hoose et al., 2010a), 164Tg/yr (all PBAP types, Mahowald et al., 2008)
14 and 312Tg/yr (bacteria, fungal spores and pollen, Jacobson and Streets, 2009). On the other
15 hand, measurements of continental boundary layer air in remote vegetated regions indicate
16 that the mass fraction of PBAP in the coarse particle size range can be as high as $\sim 30\%$
17 ($>0.2 \mu\text{m}$, Siberia, Matthias-Maser et al., 2000) or $65\text{-}85\%$ ($>1 \mu\text{m}$, Amazonia, Martin et al.,
18 2010; Pöschl et al., 2010; Huffman et al., 2012).

19 Like all other aerosol particles, PBAP can influence the Earth's climate by forcing the
20 radiation budget directly (by absorbing or scattering radiation) and indirectly (by affecting
21 cloud microphysics) (Forster et al., 2007). The direct PBAP effect on climate is difficult to
22 estimate, because atmospheric PBAP concentrations can vary by several orders of magnitude
23 depending on time and location. Describing the radiative properties of PBAP is complicated,
24 because their size ranges from fine to coarse (up to $100 \mu\text{m}$ in diameter) and in many cases
25 their shapes are non-spherical and not accurately known. Hence, the applicability of Mie
26 scattering theory is limited (Després et al., 2012). However, the direct PBAP effect on global
27 and regional climate is generally assumed to be small due to low average concentrations, in
28 contrast to the numbers of sub-micron absorbing and scattering aerosols. The indirect PBAP
29 effect on climate is caused by PBAP that act as cloud condensation nuclei (CCN) and/or as
30 ice nuclei (IN). Generally, changing aerosol populations (e.g. increasing nuclei concentrations
31 or behavior) can alter the microphysical properties of clouds, thus influencing the climate
32 system (Forster et al., 2007). Most PBAP are assumed to be good CCN, because their surface

1 area is large compared to most other aerosol species (Petters and Kreidenweis, 2007; Ariya et
2 al., 2009) and thus may act as so-called giant CCN (Pöschl et al., 2010). For these particles,
3 the Kelvin effect can be neglected when describing water vapor condensation, and thus
4 activation and growth proceeds quickly (Pope, 2010). Some particles of biological origin (e.g.
5 *P. syringae* bacteria and some fungal species) have been found to efficiently nucleate ice
6 growth at relatively high temperatures (Després et al., 2012; Murray et al., 2012; Hoose and
7 Möhler, 2012; Morris et al., 2004; Morris et al., 2013; Haga et al., 2013). Biological particles
8 have been observed ubiquitously in precipitation, fog, and snowpack (e.g. Christner et al.,
9 2008) and in clouds by airborne measurements (e.g. Prenni et al., 2009; DeLeon-Rodriguez et
10 al., 2013) and have been shown to be important fractions of IN measured at ground level (e.g.
11 Huffman et al., 2013; Prenni et al., 2013). These bio-IN may be important for ice nucleation
12 in mixed-phase clouds at temperatures higher than -15°C (DeMott and Prenni, 2010). In
13 regimes colder than that, mineral dust particles and other ice nucleators are also active and the
14 relative atmospheric abundance of PBAP is probably too small to contribute significantly to
15 formation and evolution of these colder clouds. Previous modelling studies suggest that bio-
16 IN concentrations are several orders of magnitude lower than IN concentrations from mineral
17 dust or soot and hence the influence of bio-IN on precipitation is limited on the global scale
18 (Hoose et al., 2010a; Sesartic et al., 2012; Spracklen and Heald, 2013). *In-situ* analyses of
19 insoluble cloud ice and precipitation residuals meanwhile highlight the contribution of bio-IN
20 to precipitation, and back trajectories indicate that they can be transported over large distances
21 (Creamean et al., 2013).

22 The methods for identifying and detecting PBAP are challenging and many different PBAP
23 can introduce significant detection biases. Particle diameter often plays heavily into PBAP
24 detection and characterization, and it should be noted that large discrepancies can exist
25 between physical and aerodynamic diameter measurements (Huffman et al., 2010; Reponen et
26 al., 2001). PBAP concentrations can be obtained either by online techniques, in which
27 samples are analyzed by advanced instrumentation in real-time, or by offline measurement
28 techniques. If measured offline, samples of airborne biological particles are stored under
29 refrigeration and common methods include analysis by microscopy (stained or unmodified),
30 by cultivation of the sample on growth media, and by amplification and detection of genetic
31 material by sequencing or electrophoretic separation. Chemical and optical properties of
32 PBAP samples or their tracers can be monitored in real time by: chromatography, mass
33 spectrometry, fluorescence spectrophotometry, LIDAR, and flow cytometry. Short overviews

1 of PBAP analysis techniques have been given by Caruana et al. (2011) and Després et al.
2 (2012).

3 This paper focuses on the mesoscale simulation of atmospheric concentrations of fungal
4 spores. A limited-area model is used for the simulations and the setup includes a model
5 domain covering most parts of Europe with a horizontal resolution of 14 km. Two different
6 fungal spore emission parameterizations (Heald and Spracklen, 2009; Sesartic and Dallafior,
7 2011) are tested by comparing their number concentrations to online laser-induced
8 fluorescence (LIF) measurements of airborne fluorescent biological particles. Additionally, a
9 new emission parameterization adapted to these measurements is introduced. Field data used
10 here comes from a real-time measurement technique that detects the intrinsic (i.e. unstained)
11 fluorescence signal, after UV excitation, of fluorophores commonly present in most biological
12 materials (e.g. free proteins, fungal spores, bacteria, and leaf fragments). Detected particles
13 are categorized as fluorescent biological aerosol particles (FBAP), which may broadly be
14 considered a lower limit for the abundance of PBAP (Huffman et al., 2010; Pöhlker et al.,
15 2012; Healy et al., 2014). FBAP were measured at four different locations (Table 1)
16 concurrently during three focus periods in summer 2010 and fall 2010. The resulting FBAP
17 size distribution is usually dominated by particles in the range from 2 μm to 4 μm , which is
18 consistent with the size of fungal spores (Huffman et al., 2010; Pöschl et al., 2010; Huffman
19 et al., 2012; Healy et al., 2012a; Toprak and Schnaiter, 2013; Huffman et al., 2013). Further,
20 the concentration of FBAP in a given air-mass is generally considered to underestimate PBAP
21 concentration due to biological particles that exhibit very low levels of fluorescent emission
22 (Huffman et al., 2012). To some extent, non-biological aerosol components can also be part of
23 the fluorescence signal for fine particles ($\sim 1 \mu\text{m}$) (Huffman et al., 2010; Toprak and
24 Schnaiter, 2013). These factors contribute uncertainty to the evaluation of the
25 parameterizations discussed here, however the overall ability of LIF techniques to provide
26 real-time FBAP measurements allows first approximation measurements that can be
27 enlightening.

28

1 2. Methodology

2 2.1. Model Description

3 The COSMO-ART (Consortium for Small-scale Modelling – Aerosols and Reactive Trace
4 gases) atmospheric model system is based on the forecast model of the German weather
5 service, combined with an online coupled module for simulating the spatial and temporal
6 distribution of reactive gaseous and particulate components (Vogel et al., 2009). Additionally,
7 fungal spores are incorporated as an independent, monodisperse particle class ($d_p = 3 \mu\text{m}$).

8 Parameterizations for emission, sedimentation, and washout, which were originally developed
9 for pollen dispersal, are included for this particle class (Helbig et al., 2004). Fungal spores are
10 treated independently, as no interactions with other aerosols or gases (coagulation or
11 condensation) are considered. The temporal development of the fungal spore number
12 concentration is calculated by:

$$\rho \frac{d\Psi}{dt} = -\nabla \cdot \vec{F}_T - \frac{\partial}{\partial z} F_S - \lambda \Psi - \frac{1}{N} \frac{\partial}{\partial z} F_E \quad (1)$$

13 with the number mixing ratio of fungal spores being

$$\Psi = \frac{N_f}{N}, \quad (2)$$

14 and the number concentration of fungal spores N_f , the total number of particles and air
15 molecules N per m^3 , the air density ρ , the turbulent flux \vec{F}_T , the sedimentation flux F_S , a
16 washout coefficient λ and a vertical emission flux F_E (Vogel et al., 2008). The turbulent flux
17 is calculated by $\vec{F}_T = \overline{\rho v' \Psi'}$, incorporating the turbulent fluctuations of wind speed v' and
18 fungal spore number mixing ratio Ψ' . Fungal spore sedimentation is calculated by
19 $F_S = \rho \Psi v_s$. The fungal spore settling velocity v_s is calculated by applying the volume-
20 equivalent particle diameter $d_e = 2 \sqrt[3]{a^2 b}$, with $a = 1 \mu\text{m}$ and $b = 5 \mu\text{m}$ (Yamamoto et al.,
21 2012) being the major and minor radius of a prolate spheroid. This results in:

$$v_s^2 = \frac{4 \rho_p d_e g}{3 \rho c_d} \quad (3)$$

22 where $\rho_p = 1 \text{ g/cm}^3$ is the spore density (Trail et al., 2005; Gregory, 1961) and c_d the drag
23 coefficient (Aylor, 2002). The calculation of the washout coefficient is based on the
24 assumption of raindrops being much larger than aerosol particles and having a much higher
25 terminal fall velocity. It yields:

$$\lambda(d_p) = \int_0^{\infty} \frac{\pi}{4} D_D^2 v_t(D_D) E(d_p, D_D) n(D_D) dD_D \quad (4)$$

1 (Rinke, 2008). D_D and d_p are the diameters of raindrops and particles, respectively, $v_t(D_D)$ is
 2 the terminal fall velocity, E is a collision efficiency and $n(D_D)$ is the size distribution of the
 3 raindrop number concentration. For fungal spores with a spherical diameter of 3 μm , the
 4 collision efficiency E with 0.1 mm and 1 mm droplets is approximately 0.085 and 0.3,
 5 respectively.

6 Adapting the model for simulations of fungal spores requires inclusion of an emission flux F_E
 7 in the source term of eq. (1) by means of an emission parameterization which will be
 8 described in the next section.

9 Together with fungal spore simulations COSMO-ART is used to compute the mass
 10 concentration of major atmospheric aerosol components. Hence, the proportion of fungal
 11 spores with respect to the dry aerosol mass can be estimated (section 3.4). In addition to
 12 primary aerosol emissions, further gaseous emissions (section 2.3) are taken into account.
 13 Partitioning of inorganic aerosol components between the gases and particulate phase is
 14 simulated by the ISORROPIA II module (Fountoukis and Nenes, 2007). Condensation on
 15 fungal spore aerosols is not included. The contribution of secondary organic aerosols (SOA)
 16 to the particles is handled by condensation of oxidized volatile organic compounds as
 17 described by Schell et al. (2001). When soot aerosols are not involved as a solid nuclei
 18 enabling condensation, clusters build by gas-to-particle conversion via binary nucleation of
 19 sulfuric acid and water. They are computed as an individual particle mode. All aerosol
 20 particles including these chemical compounds are assumed to be internally mixed. A soot
 21 mode without mixing of other chemical compounds is included as particles that are emitted
 22 directly into the atmosphere. Anthropogenic primary aerosols (aPA) in the coarse size range
 23 ($<10 \mu\text{m}$) are treated as a separate mode. Detailed descriptions are given in Vogel et al.
 24 (2009). Furthermore, sea salt is included in the model simulation and its emission is related to
 25 sea water temperature and wind speed (Lundgren et al., 2013). No desert dust emissions are
 26 included, as the model domain does not cover the corresponding emission regions and no
 27 transport into the model domain is taken into account.

28

1 2.2. Emission Parameterization of Fungal Spores

2 In previous studies, a constant emission rate was used as input of a global chemical transport
3 model to represent the magnitude and range of measured concentrations of mannitol as a
4 molecular tracer for basidiospores (Elbert et al., 2007). Broad geographical differences can be
5 included in the emission flux by distinguishing between ecosystems. While reviewing the
6 measured data available on measured fungal spore concentrations, Sesartic and Dallafior
7 (2011) calculated number fluxes of fungal spore emissions for six different ecosystems
8 (defined by Olson et al., 2001). Four of these emission fluxes were included into
9 COSMO-ART, and coupled to ecosystem definitions by the GLC2000 (Global Landcover
10 2000 Database) (forest and shrubs) and Ramankutty et al. (2008) (grassland and crops). The
11 sum of these fluxes, as defined by Sesartic and Dallafior (2011), are emitted from the land
12 area fraction E_i of each ecosystem i ($\sum_i^n E_i = 1$ for n number of ecosystems), gives the total
13 emission flux $F_E = F_{S\&D}$ in $\text{m}^{-2}\text{s}^{-1}$ of eq. (1) for fungal spores:

$$\begin{aligned} F_{S\&D} = & 214 \text{ m}^{-2}\text{s}^{-1}E_{forest} + 1203 \text{ m}^{-2}\text{s}^{-1}E_{shrub} + 165 \text{ m}^{-2}\text{s}^{-1}E_{grassland} \\ & + 2509 \text{ m}^{-2}\text{s}^{-1}E_{crop} \end{aligned} \quad (5)$$

14 Additionally, a second emission parameterization was tested, which varies as a function of
15 meteorological and surface conditions. Jones and Harrison (2004) reviewed the relations
16 determined when analyzing the observed fungal spore concentrations and atmospheric factors.
17 Seasonal variations can be explained by changes in the leaf area index (LAI). This was
18 verified by correlation to the observed mannitol concentrations. Among the drivers of day-to-
19 day variations, specific humidity (q_v) correlates best with the mannitol concentrations (Heald
20 and Spracklen, 2009). It was argued that though other atmospheric factors (e.g. temperature)
21 may actually drive the correlation, this does not change correlation results and thus
22 parameterizations can proceed without having information about the root drivers of fungal
23 spore release. The emission rate is linearly scaled with LAI and q_v in order to give global
24 fungal spore concentrations matching the mean mannitol concentrations (Heald and
25 Spracklen, 2009). In order to rescale the emission flux specified in Hoose et al. (2010a) from
26 a spore diameter of $5 \mu\text{m}$ as in Hoose et al (2010a) to a spore diameter of $3 \mu\text{m}$ as in this
27 study, the prefactor c is set to $c = 2315 \text{ m}^{-2} \text{ s}^{-1}$. Based on the emission flux in eq. (1), this
28 gives an alternative source $F_E = F_{H\&S}$ of fungal spores in $\text{m}^{-2}\text{s}^{-1}$:

$$F_{H\&S} = c \frac{LAI}{5 \text{ m}^2 \text{ m}^{-2}} \frac{q_v}{1.5 \times 10^{-2} \text{ kg kg}^{-1}} \quad (6)$$

1 *LAI* is the leaf area index, q_v is the specific humidity at the surface. In the COSMO-ART
 2 simulations *LAI* is horizontally distributed according to GLC2000 containing monthly
 3 variation and q_v is provided by the model as a meteorological variable.

4

5 **2.3. Model Domain and Input Data**

6 The COSMO-ART mesoscale model system is driven by initial and boundary data for
 7 meteorological conditions. They are updated every six hours and result from interpolation of
 8 the coarse grid operational atmospheric model analysis of the ECMWF (European Centre for
 9 Medium-Range Weather Forecasts). No initial and boundary concentrations are predefined for
 10 aerosols or gases. Therefore, all gaseous species are set to a climatological, homogeneously
 11 distributed initial concentration and emission rates for chemical compounds included in the
 12 ART part are updated hourly. They are provided by EMPA (Swiss Federal Laboratories for
 13 Materials Science and Technology) based on the TNO/MACC (Monitoring Atmospheric
 14 Composition and Climate) inventory (Kuenen et al., 2011). The treatment of emissions for
 15 COSMO-ART can be found in Knote et al. (2011). Homogeneously distributed mass densities
 16 for each aerosol are used as initial conditions, together with the aerosol size distribution and
 17 particle density. Primary particle emissions are included as parameterizations based on
 18 meteorological and surface conditions. Land use data and constant surface properties are
 19 derived from the GLC2000 database (Bartholomé and Belward, 2005). All parameters are
 20 post-processed to the rotated spherical coordinate system of COSMO-ART (Doms and
 21 Schättler, 2002). For the purpose of this paper, the model domain covers most parts of
 22 Western Europe from mainland Portugal to northern Finland, the longitudinal extension being
 23 2849 km the latitudinal extension being 3803 km with a horizontal spacing of 0.125°
 24 ($\triangleq 14$ km) on a rotated grid. In vertical direction the model reaches up to an altitude of about
 25 24 km distributed over 40 terrain-following levels. The timestepping of the Runge-Kutta
 26 dynamical core is set to 30 s.

27

1 **2.4. Auto-fluorescence Measurements**

2 Ambient aerosols can be roughly classified as biological or not by interrogating particles at
3 characteristic wavelengths of excitation and measuring the resultant emission in a process
4 called ultraviolet light-induced fluorescence (UV-LIF) (e.g. Hairston et al., 1997; Pan et al.,
5 1999). In particular, the region of fluorescent excitation near 360 nm is often used as
6 characteristic of certain cell metabolites present in all living cells, including riboflavin and
7 reduced pyridine nucleotides (e.g. NAD(P)H). The region of excitation near 270 nm includes
8 certain amino acids (e.g. tryptophan) contained in most proteins. However, many other
9 biological fluorophores exist and the relationship between the measured fluorescence of
10 complex biological particles and fluorophore assignment is very complex (Pöhlker et al.,
11 2012; Pöhlker et al., 2013).

12 Two instrument types were utilized at four locations for the comparison discussed in this
13 paper. The ultraviolet aerodynamic particle sizer (UV-APS; TSI, Inc., Shoreview, MN, USA)
14 measures particle size aerodynamically, excites individual particles using a single Nd:YAG
15 laser pulse at 355 nm, and detects integrated fluorescent emission (non-dispersed) in a single
16 wavelength region between 420 nm and 575 nm (Hairston et al., 1997; Brosseau et al., 2000;
17 Huffman et al., 2010). The Waveband Integrated Bioaerosol Sensor (WIBS, versions 3 and 4;
18 University of Hertfordshire, UK) measures particle size optically and excites individual
19 particles via two sequential pulses from a Xe-flash lamp, at 280 nm and 370 nm,
20 respectively (e.g. Kaye et al., 2005; Foot et al., 2008). Fluorescence for each particle is then
21 measured in one of two wavelength regions, resulting in three measured fluorescence
22 parameters for each WIBS instrument named FL1_280, FL2_280, and FL3_370. See Gabey
23 et al. (2010) and Robinson et al. (2013) for more details, including slight differences in
24 WIBS-3 and WIBS-4 models. The number concentration of FBAP can be written as $N_{F,c}$ with
25 subscripts referring to fluorescent and coarse particle size. The differences in the pairs of
26 wavelengths used for fluorescence, as well as the possible differences in sensitivity between
27 instruments, suggest that the term “FBAP” as determined by each instrument is not rigorously
28 interchangeable, and it is critical to understand the method of analysis when comparing
29 datasets. For example, the ambient FBAP number concentration as determined by UV-APS
30 has been shown to be qualitatively consistent with the number concentration of particles that
31 fluorescence in the WIBS FL3_370 channel, while the $N_{F,c}$ comparison between UV-APS and
32 WIBS FL1_280 channel is relatively poor (Healy et al., 2014). Here we use the term FBAP

1 from WIBS data to mean particles that exhibit fluorescence simultaneously in both channels
2 FL1_280 and FL3_370.

3 Particle size can aide differentiation between biological particles classes observed, however
4 the selectivity based on size alone is very uncertain. For example, and to a rough first
5 approximation, it may be true that many FBAP $\sim 1 \mu\text{m}$ are single bacterial particles and that
6 many FBAP 2 - 6 μm may be fungal spores or bacterial agglomerates (Shaffer and Lighthart,
7 1997). A comparison between WIBS-4 and a Burkard volumetric impactor reported by
8 (O'Connor et al., 2014) from a yew forest site showed excellent correlation with $R^2 > 0.9$
9 demonstrating the real-time counting capability of WIBS for pollen. However, biological
10 species can vary widely, and other FBAP classes (e.g. fragments of larger PBAP, internal
11 components of burst pollen, the presence of other biological species) confound the simple
12 assignment of FBAP based on size (Després et al., 2012).

13 Further, at least a fraction of fluorescent, supermicron particles are likely to come from non-
14 biological sources, and thus could be counted as FBAP. These non-biological process include
15 anthropogenic sources (e.g. polycyclic aromatic hydrocarbon particles from combustion and
16 cigarette smoke), present most often in submicron particles (Huffman et al., 2010), select
17 oxidized organic aerosol particles (e.g. absorbing brown carbon particles) (Bones et al., 2010;
18 Lee et al., 2013), and some humic-like substances (Gabey et al., 2013). For example, at the
19 rural, elevated site of Puy de Dôme, France, WIBS-3FBAP measurements were compared to
20 results from fluorescence microscopy paired with staining of fungal spores and bacteria.
21 These results suggest that the real-time UV-LIF measurements indeed track the diurnal cycle
22 of the bacteria concentration, but that non-biological particles still contributed significantly to
23 fluorescent particle number (Gabey et al., 2013).

24 Virtually every ambient measurement study performed with the WIBS or UV-APS to date has
25 shown a dominant FBAP mode peaking at 2 - 4 μm in size (Huffman et al., 2010; Huffman et
26 al., 2012; Huffman et al., 2013; Gabey et al., 2010; Toprak and Schnaiter, 2013; Healy et al.,
27 2014). For example, the FBAP size distributions measured at each of the four sampling
28 locations discussed here is shown in Figure 1, highlighting the common presence of the
29 2 - 4 μm peak. It has been proposed that fungal spores and bacteria agglomerates are the most
30 dominant biological aerosols in this size range (Jones and Harrison, 2004; Després et al.,
31 2012; Fang et al., 2008) and that the FBAP signal in this size range is typically dominated by
32 fungal spores. This was corroborated in more detail for a remote Amazonian site using FBAP

1 analysis along with fluorescence microscopy of stained filter samples (Huffman et al., 2012),
2 but has not yet been rigorously tested in other environments. At the costal site of Killarney,
3 results of fluorescence and optical microscopy of impacted biological particles reveal that
4 some PBAP, e.g. spores of *Cladosporium spp.*, which have been frequently observed in many
5 environments, were not correlated to the FBAP concentration (Healy et al., 2014). However,
6 particle size modes of WIBS channel FL2_280 correlate with the concentration of airborne
7 fungal spores commonly observed at the sampling site (Healy et al., 2014). Other microscopy
8 and DNA-based studies have suggested that fungal spores constitute the largest fraction of
9 PBAP in the 2 – 4 μm size (e.g. Graham et al., 2003; Lin and Li, 1996; Burch and Levetin,
10 2002). Bauer et al. (2008) showed that fungal spores account for an average of 60% of the
11 organic content in the particulate matter in a size range of 2 - 10 μm in rural and urban areas
12 of Vienna, Austria.

13

1 3. Results

2 3.1. Comparison of Time Series of Measured FBAP and Simulated Fungal 3 Spores

4 Fungal spore concentrations simulated using the emission fluxes given in eqs. (5) and (6)
5 according to Sesartic and Dallafior (2011) and Heald and Spracklen (2009) were first
6 compared to FBAP measurements without further adjustment. An overview of time series for
7 all measurements and simulations discussed here is shown in Figure 2 by a box-and-whiskers
8 plot. Statistical parameters of the correlation between observations and simulations are
9 presented in Table 2. The time periods for each of three case studies (Table 1) were chosen as
10 exemplary periods when UV-LIF instruments were operating simultaneously at a minimum of
11 two locations, with no requirements applied with respect to environmental conditions. For the
12 statistical analysis, FBAP measurements were averaged over one hour periods in order to be
13 consistent to the model output time steps. The correlation coefficient for the entire data set
14 amounts to $R = 0.43$ for the simulation with the (Heald and Spracklen, 2009) emission ($F_{H\&S}$)
15 and to $R = -0.05$ for the simulation with the (Sesartic and Dallafior, 2011) ($F_{S\&D}$)
16 parameterization. For most time periods at Karlsruhe and Hyytiälä, the simulated fungal spore
17 concentrations are smaller than the measured FBAP concentrations (Figure 2). This difference
18 is highest at Hyytiälä in August 2010. At Hyytiälä in July and at Manchester and Killarney in
19 August, $F_{H\&S}$ gives median concentration values which agree reasonably well with the
20 measurements. During October, the fungal spores number concentrations based on constant
21 emission fluxes ($F_{S\&D}$) agree best with the measured FBAP concentrations. Taking the whole
22 dataset together, these deviations result in negative values of the normalized mean bias (NMB)
23 of -44% for $F_{H\&S}$ and of -29% for $F_{S\&D}$ and root mean square errors of 26.2 L^{-1} and 25.6 L^{-1} ,
24 respectively (Table 2). Possible causes for the bias of $F_{H\&S}$ and $F_{S\&D}$ may come from different
25 assumptions made to determine the fungal spore concentrations in ambient air. On the one
26 hand, the mass size distribution of mannitol, which is used as a chemical tracer for fungal
27 spores by Heald and Spracklen (2009), peaks in their study at particle diameters of $\sim 5 \mu\text{m}$.
28 Additionally to fungal spores, bacteria, algae, lichens, and plant fragments, can produce
29 mannitol and some of these can contribute to PBAP concentrations at $\sim 5 \mu\text{m}$. On the other
30 hand, similar assumptions are made for this study by linking FBAP to fungal spores, which
31 can also introduce biases. Furthermore, the treatment of fungal spores as monodisperse

1 particles in the model (while the observed size distribution is rather broad) influences the
2 simulated removal processes and thus the resulting concentrations.

3 Long-term analysis of FBAP measurements, including periods at the Karlsruhe (Toprak and
4 Schnaiter, 2013) and Hyytiälä site (Schumacher et al., 2013) discussed here, shows an annual
5 cycle of average FBAP number concentrations peaking in summer and lowest in winter. Thus,
6 a simulation based on a constant emission flux (such as $F_{S\&D}$) may not be appropriate to
7 reproduce the seasonal variation in FBAP concentrations, contributing to the low value of R .

8 Figures 3 to 6 show a series of one-week long case studies, each representing two
9 measurement sites. The plots show comparisons between simulation and measurement time
10 series for each station. The simulated fungal spore number concentration is given for the
11 model grid point closest to the measuring site. Due to model spin-up, the first six hours of the
12 simulated fungal spore concentrations are removed from the figures and are not included in
13 the analysis. The total precipitation calculated by the model is shown by gray bars with the
14 ordinate on the right hand side of the figure. The simulated boundary layer height is also
15 included at the bottom of each panel in the figures.

16 Measured FBAP number concentrations often exhibit distinct diel (24-h) cycles with a
17 maximum in the morning hours or around midnight and a minimum around noon. These
18 features have been consistently reported by most studies discussing temporal behavior of
19 FBAP (Gabey et al., 2010; Huffman et al., 2010; Huffman et al., 2012; Toprak and Schnaiter,
20 2013). Here, a similar diel cycle is frequently obtained from simulations, and the simulated
21 fungal spore concentrations often anti-correlate with the simulated boundary layer height
22 (h_{PBL}) (Figures 3 to 6). The measured FBAP concentrations often qualitatively track the
23 general pattern of simulated h_{PBL} , however the magnitude of concentration change and the
24 timing is often not consistent. For example, on 24 and 25 July at the Karlsruhe site (Figure 3a)
25 a boundary layer compression during the night leads to an increase in the simulated fungal
26 spore concentrations by a factor of ~ 4 , and during day the concentrations decreases as the
27 boundary layer rises again. In this case, the measured FBAP concentrations are in relatively
28 good agreement with the simulated fungal spore numbers, with $N_{F,c}$ dropping slowly during
29 the day on 24 and 27 July, and to a rate closer to the simulations on 25 July. This suggests that
30 FBAP concentrations were likely influenced, at least partially, by the changing boundary
31 layer height, though diel changes in biological emission are also likely to influence diel FBAP
32 patterns. A similar temporal pattern in simulated fungal spore concentrations is shown in

1 Figure 4a, where a maximum in h_{PBL} at 12 and 13 October occurs approximately coincident
2 with a minimum in the simulated number concentration. In this case, however, the measured
3 FBAP concentrations do not reflect the diel pattern of the simulations. On 31 August (Figure
4 5a), measured FBAP and simulated fungal spore number concentration increase
5 simultaneously and parallel to the boundary layer compression, but the increase is more
6 intense for FBAP measurements than for spore simulations. Additionally, at Manchester
7 between 31 August and 1 September (Figure 6a) measured and simulated concentrations are
8 in good agreement. Distinct minima and maxima clearly anti-correlate with the minima and
9 maxima of the boundary layer height. Similarly, during the same time period in Killarney
10 (Figure 6b), changes in the boundary layer height were simulated along with coincident
11 changes in fungal spore concentrations. In contrast, Figures 4a, 4b, and 5b show diel FBAP
12 concentration changes that correlate poorly with simulated h_{PBL}^{-1} .

13 For a more quantitative analysis, the correlation coefficient between N_f and h_{PBL}^{-1} was
14 calculated for the whole dataset (Table 3). The resulting value is a small positive correlation
15 of $R = 0.11$ with a 95% confidence interval between 0.05 and 0.17. If all data points with
16 simulated boundary layer heights below 10 m (which are considered problematic as the
17 vertical resolution of the model is coarser than 10 m) are omitted from the correlation
18 analysis, the correlation coefficient rises to $R = 0.18$ with a 95% confidence interval between
19 0.12 and 0.24. The correlation coefficients for the individual time series are also listed in
20 Table 3. Note that a large positive correlation cannot be expected, as variations in the
21 emission flux, deposition processes and transport all lead to a reduction of the correlation
22 between N_f and h_{PBL}^{-1} . Three of the stations exhibit negative correlation coefficients, which
23 might be due to perturbations by rain as discussed below.

24 We conclude that (i) simulated fungal spore concentrations are sensitive to changes in the
25 simulated boundary layer height, by extension, that (ii) diel cycles of FBAP concentrations
26 are likely to be partially influenced by diel cycles of boundary layer height, but that (iii) the
27 development of the FBAP concentration is in addition influenced by daily cycles in biological
28 emission processes, including those of fungal spores and other PBAP classes, and
29 atmospheric transport and sink processes. These competing effects are ~~impossible~~ difficult to
30 separate when only point measurements are available.

31 A comparison of measured FBAP and simulated fungal spore number concentrations for July
32 2010 is shown in Figure 3. At the measurement site of Karlsruhe, diel cycles were found in

1 the simulated and measured time series, with constantly lower concentrations being obtained
2 from simulations based on emission parameterizations given in literature. When precipitation
3 occurs in the simulation, the simulated fungal spore concentrations decrease due to washout
4 and the diel development of the concentration is interrupted. Afterwards, the simulated
5 concentrations quickly return to the previous baseline. At Hyytiälä a strong decrease in
6 simulated fungal spore concentration on 24 July precisely overlaps with the simulation of
7 precipitation. After hitting a minimum value during simulated precipitation, the simulated
8 fungal spore concentration increases steadily for two days as a result of a post-frontal shift in
9 wind direction and decrease in wind speed. The increase is also reflected in the measured
10 FBAP concentrations. However, the simulated precipitation values do not always coincide
11 with precipitation at the site, as was the case in this instance. As a result of no rain falling at
12 the site on 24 July, the measured FBAP concentration was not affected by washout as in the
13 simulations. This example shows that errors in the simulated meteorology contribute to
14 uncertainty in the simulated aerosol concentrations. Additionally, other dynamic processes are
15 known to affect FBAP concentrations. For example, FBAP has been shown to increase
16 dramatically during rainfall, a process reported recently for both a site in Colorado (Huffman
17 et al., 2013) and also at the Hyytiälä site (Schumacher et al., 2013). The reasons for this
18 FBAP increase are unclear, but are thought to be related to mechanical ejection from
19 terrestrial surfaces as a result of rain droplet splash (Huffman et al., 2013). These effects are
20 known to be dependent on the local geography and ecology, however, and are outside the
21 scope of the presented emission parameterizations.

22 During the simulation period of October 2010, the simulated fungal spore number
23 concentrations $F_{H\&S}$ are consistently below the measured FBAP concentrations at the sites of
24 Karlsruhe and Hyytiälä, whereas $F_{S\&D}$ matches the relative magnitude of the measurements
25 more closely in both cases (Figure 4). At Karlsruhe, concentrations simulated by each
26 emission parameterization follow a distinct diel cycle and increase slightly through the week,
27 reaching concentration maxima on 15 October. The measured FBAP concentration develops
28 differently, with only very weak diel cycle present from 11 to 14 October, and showing little
29 relationship to the simulated h_{PBL} , as discussed above.

30 At the end of August 2010, four different measurement series were available for a comparison
31 to fungal spore simulations (Figure 5 and 6). The measured time series of FBAP number
32 concentrations generally exhibit diel cycles, as discussed. The absolute FBAP concentration

1 at Hyytiälä was consistently highest, when comparing all four sites. This trend is even more
2 obvious when comparing the median concentrations on a linear scale (Figure 2).
3 Concentrations simulated from the literature-based parameterizations under-predict
4 measurements by the greatest margin at Hyytiälä. This under-prediction is likely a result of
5 particle washout due to the persistent precipitation simulated by the model and is an
6 indication that precipitation has a stronger influence on the simulated concentrations than
7 changes in the boundary layer height. Measured rainfall during this period at Hyytiälä was
8 less continuous than the model predicts, but occurred with episodic peaks. In all other August
9 case studies, simulated fungal spore concentrations show relatively good agreement with
10 FBAP measurements.

11

12 **3.2. Development of a new FBAP Emission Parameterization by Adaptation to** 13 **FBAP Measurements**

14 Direct comparison between simulated fungal spores and measured FBAP reveals that in
15 general the simulated concentrations are lower than the measured concentrations (Figure 8a).
16 This difference is most distinct at Hyytiälä during the August case study and at Karlsruhe in
17 the July and October case studies. Here we suggest a new parameterization, including
18 meteorological and surface parameters identified earlier, as drivers of emissions of FBAP,
19 which may in many cases be comparable to fungal spores. In the model, FBAP are treated
20 identically to fungal spores as described in section 2.1. Additionally, new parameters driving
21 FBAP emissions have been investigated. The emission flux depends on these parameters and
22 their fitting coefficients obtained from a regression analysis of the FBAP measurements as
23 described below. The new parameterization for FBAP emissions has been incorporated into
24 COSMO-ART and the resulting concentrations are included in Figures 3 to 6.

25 The adjusted parameterization for the emission flux is based on a regression analysis of an
26 emission flux $F_{F,c}$ estimated from the FBAP number concentration. For this, it is assumed that
27 particles are evenly distributed throughout the planetary boundary layer and that the simulated
28 FBAP concentration correlates with h_{PBL}^{-1} . This assumption is expected to be fulfilled best for
29 days with a cloud-free convective boundary layer. Together with a steady-state condition and
30 neglecting horizontal exchanges with the surrounding air, the balance holds between the
31 number concentration (N_f) and the emission rate ($F_{F,c}$) together with the atmospheric lifetime
32 of FBAP (τ):

$$N_f = \frac{F_{F,c}\tau}{h_{PBL}} \quad (7)$$

1 (Seinfeld and Pandis, 2006). The boundary layer height at the measurement site needs to be
 2 taken from the model simulation as it is not measured consistently. Eq. (7) is applicable to
 3 derive estimates for $F_{F,c}$ under the assumption that the variation of the simulated boundary
 4 layer height explains a significant amount of the variation in N_f . This condition is fulfilled for
 5 four of the individual time series and to a lesser extent for the dataset as a whole (see section
 6 3.1 and Table 3).

7 In eq. (7), the FBAP lifetime τ represents a boundary layer ~~mixing residence~~ time ~~and is not~~
 8 ~~identical to an atmospheric residence time~~. For an initial test simulation, τ ~~was~~ assumed to be
 9 constant and ~~is~~ estimated with an initial value of one day, as given in literature for
 10 atmospheric lifetimes of aerosol particles with 3 μm in diameter (Jaenicke, 1978). In this ~~test~~
 11 ~~casesimulation~~, the ~~resulting~~ FBAP concentrations ~~with the initial value of atmospheric~~
 12 ~~lifetime reveals an underestimation~~ ~~were a about factor of 5 lower~~ compared to the FBAP
 13 measurements. As a remedy, τ is ~~heuristically corrected adjusted~~ to $\tau = 4 \frac{3}{4}$ hours, ~~such that~~
 14 ~~the simulated concentrations on average match the observed concentrations~~ ~~which can be~~
 15 ~~understood as a mean time for boundary layer mixing of FBAP~~. The deviation from a lifetime
 16 of 3 μm particles given in literature may be attributed to ~~different factors, like~~ the ~~assumption~~
 17 ~~of a constant vertical~~ ~~vertical variation of the distribution concentration~~ of fungal spores ~~with~~
 18 ~~increasing altitude until boundary layer height~~ ~~within the boundary layer (example shown in~~
 19 ~~Figure 7)~~. ~~A typical vertical profile from the model (Figure 7) shows that this assumption is~~
 20 ~~valid as a first approximation, but that deviations are visible both close to the surface and~~
 21 ~~close to the top of the boundary layer. In the simulations, a mean ratio of approximately 1.75~~
 22 ~~between surface level concentrations and mean concentrations within the boundary layer is~~
 23 ~~found. This ratio is still too small to explain the discrepancy between the expected lifetime~~
 24 ~~and the value of $\tau = 4 \frac{3}{4}$ hours which leads to agreement with the observed concentrations~~
 25 ~~from which the emission flux was derived. The remaining discrepancy may be caused by~~ the
 26 broad size distribution of FBAP particles (see Figure 1), advection processes, non-equilibrium
 27 conditions, and ~~the exchange with the free troposphere and~~ the much longer lifetime of spores
 28 above the boundary layer.

29 Two types of instruments operating with different numbers of channels and detecting
 30 fluorescence at different wavelengths are used here for deriving an emission parameterization

1 appropriate for fungal spores. The technical difference may lead to significantly different
2 FBAP concentrations (Healy et al., 2014), because the WIBS instrument only counts particles
3 as FBAP when a signal exceeds a threshold in both channels (Pöhlker et al., 2012; Gabey et
4 al., 2010). Some fungal spores most abundant in the Earth's atmosphere and very common for
5 fungal spores of 2 - 4 μm (*Cladosporium sp.*, *Aspergillus versicolor*, *Penicillium solitum*)
6 (Fröhlich-Nowoisky et al., 2012; Hameed and Khodr, 2001) only show a weak signal in the
7 emission wavelength of 310 nm to 400 nm (Saari et al., 2013; Healy et al., 2014). This
8 difference needs to be taken into account when comparing absolute concentrations of fungal
9 spores and FBAP. During the time periods shown here, the WIBS indicate slightly lower
10 FBAP concentrations than the UV-APS when comparing to the model results. In general, this
11 feature is not always valid and detailed side-by-side comparisons between the two types of
12 instruments are required to determine their behavior in terms of FBAP detection and
13 estimation of the PBAP concentration. In the attempt to factor out the technical difference
14 between the instruments, we assume that the FBAP concentration can be multiplied by a
15 constant factor for the concentration values to match each other. The amount of FBAP given
16 by the UV-APS may be represented best by WIBS channel FL3_370 (section 2.4). The FBAP
17 concentration given by the UV-APS is therefore reduced by a factor derived from the WIBS
18 instrument as the mean ratio between channel FL3_370 and the total FBAP concentration
19 $N_{F,c}$ (channels FL1_280 and FL3_370). The average ratio between FL3_370 and
20 FL1_280+FL3_370 obtained from the WIBS data at Karlsruhe and Manchester during the
21 study periods is 2.2. This factor is not taken into account in the comparison of the time series
22 in section 3.1, but corrected before applying eq. (7) to the UV-APS data.

23 Analyzing the meteorological and surface parameters of the model output, it was found that a
24 better correlation with the measured FBAP concentrations is achieved for specific humidity
25 rather than relative humidity, as it was reported for previous field measurements (Gabey et al.,
26 2010; Toprak and Schnaiter, 2013; Di Filippo et al., 2013). During the time period in July
27 2010, the measured FBAP concentrations vary in a narrow range of specific humidity, which
28 is not reproduced by the literature-based simulation. For this reason, the July case study was
29 removed from the regression analysis. A dependence on the *LAI* is assumed in order to take
30 the seasonal change into account and to distinguish among various regions. A combination of
31 *LAI* and specific humidity in the regression has the advantage of reducing the fitting
32 parameters. The same relation was chosen by Heald and Spracklen (2009) for the previously
33 discussed fungal spore emission parameterization. Additionally, surface temperature

1 dependence as suggested by Di Filippo et al. (2013) is indicated by the time series and
2 factored in a regression analysis. The parameters ($b_1 = 20.426$ and $b_2 = 3.93 \times 10^4$) are
3 estimated by minimizing the sum of all squared residuals and result in a multiple linear
4 regression giving an emission flux $F_E = F_{FBAP}$ in $\text{m}^{-2}\text{s}^{-1}$ fitted to FBAP measurements:

$$F_{FBAP} = b_1(T - 275.82 \text{ K}) + b_2q_vLAI \quad (8)$$

5 where T is the surface temperature in K, q_v the specific humidity in kg kg^{-1} , and LAI the leaf
6 area index in $\text{m}^2 \text{m}^{-2}$. The parameter inside the parentheses is related to an emission offset of
7 the regression and covers unknown influences. The coefficient b_2 is approximately the same
8 as the constants in the Heald and Spracklen (2009) emission for a particle diameter of $3 \mu\text{m}$
9 given in eq. (6). The additional temperature dependence in eq. (8) increases the fungal spore
10 emission for temperatures above 275.8 K and lowers the emission for temperatures below this
11 value. The multiple linear regression (eq. (8)) yields a coefficient of determination of
12 $R^2 = 0.4$.

13

14 **3.3. Results of simulations with the new emission parameterization**

15 F_{FBAP} was implemented into COSMO-ART and applied in simulations for all three episodes.
16 Note that the extrapolation of the emission parameterization to regions especially in Southern
17 Europe, where ecosystems are different than at the stations where FBAP measurements were
18 available, is uncertain and only valid under the assumption that temperature, specific humidity
19 and LAI are universal proxies for the biological and meteorological drivers of the emission
20 strength. This hypothesis should be tested by additional observations in the future.

21 Figure 9 shows the emission flux for late August 2010, following the new parameterization,
22 horizontally distributed over a model domain covering Europe. Here, averaged over land
23 areas of the domain, F_{FBAP} gives $1.03 \times 10^3 \text{ m}^{-2}\text{s}^{-1}$. During July and October, the average flux
24 is shifted to $1.4 \times 10^3 \text{ m}^{-2}\text{s}^{-1}$ and $0.4 \times 10^3 \text{ m}^{-2}\text{s}^{-1}$, respectively, mainly as a result of seasonal
25 changes of LAI and T (not shown).

26 When analyzing the temporal development of the simulated fungal spore/FBAP
27 concentrations for each time series, F_{FBAP} mostly results in a slightly higher number
28 concentration than $F_{H\&S}$ or $F_{S\&D}$ (Figures 3 to 6). This is not the case for October 2010, where
29 the F_{FBAP} -concentrations are in the range of the literature-based concentrations. A sharp

1 decrease on 15 October at Hyytiälä, which is not reflected by simulations with literature-
2 based emission fluxes, is caused by a rapid temperature change.

3 For a statistical analysis of the results, the correlation coefficient R and its confidence
4 intervals, the normalized mean bias, and the root mean square error have been calculated for
5 the simulations with the three different emission functions (Table 3). The results indicate that
6 the bias (given by the NMB) improves by the newly introduced emission function F_{FBAP} , but
7 not the correlation R between simulated FBAP and observed FBAP concentrations which
8 remains at the value of approximately 0.43 for the overall dataset. For the different time
9 periods and stations, R varies between -0.17 and 0.66 (negative at only one station).
10 Differences in R are small between $N_{H\&S}$ and N_{FBAP} , because both make use of emission rates
11 as a function of almost the same parameters (N_{FBAP} includes an additional T -dependence).
12 The bias reduction and similar R is also visible in Figure 8. Parameters b_1 and b_2 in eq. (8) are
13 chosen to give FBAP concentrations matching best with measured FBAP concentrations, thus
14 the reduction in NMB from -44% ($N_{H\&S}$) to -0.4% (N_{FBAP}). However, the bias reduction for
15 the dataset as a whole is coincident with larger positive and negative biases for 4 out of the 8
16 episodes. Therefore, at the same time, the $RMSE$ decreases only slightly from 26.2 L^{-1} ($N_{H\&S}$)
17 to 23.2 L^{-1} (N_{FBAP}). At $T = 275.82 \text{ K}$, $F_{H\&S}$ is equal to F_{FBAP} for typical values of LAI and q_v
18 and temperatures above this threshold (as it is the case for almost all locations) shift F_{FBAP} to
19 give a larger emission flux. At meteorological conditions present for the selected cases, the
20 second part of eq. (8) dominates over the first part by a factor of ~ 4 and therefore temperature
21 changes have only a secondary influence on the emission flux. Hence, R is similar for both
22 emission parameterizations. Possible reasons for the only small improvements in R and $RMSE$
23 may be biases in the input parameters to the parameterizations or model errors in the
24 processes affecting fungal spore concentrations. To investigate this, the leaf area index was
25 compared to independent observations.

26 In Table 4, the LAI from the Global Land Cover 2000 database (European Commission, Joint
27 Research Centre, 2003), which was used in the COSMO simulations, is compared to the
28 MODIS LAI product (MCD14A2, MODIS collection 5, Knyazikhin et al., 1998) which is
29 available at 1 km horizontal and 8-day temporal resolution. Both nearest neighbor pixels and
30 averages over $20 \times 20 \text{ km}$ with standard deviations are calculated. For the Karlsruhe station and
31 for Hyytiälä in July and October, a good agreement is obtained. For Hyytiälä and Manchester
32 in August, MODIS indicates a factor of approximately 2 lower LAI than assumed in our

1 simulations. For Killarney, in contrast, the MODIS LAI is about 50% higher. While this
2 possible error in LAI can explain part of the discrepancy between simulated and observed
3 FBAP concentrations for Manchester, the bias in Hyytiälä is in the opposite direction as
4 explainable by an error in LAI and thus has to be related to other error sources. In Killarney,
5 model and measurements agree rather well despite the LAI underprediction.

6 In addition, known deficiencies in the simulated boundary layer height may reduce the quality
7 of the derived fit. The boundary layer height h_{PBL} had to be taken from the model simulations
8 as it is not continuously available from observations the stations. In the COSMO model, h_{PBL}
9 is calculated by a bulk Richardson number method (Szintai and Kaufmann, 2008). It was
10 shown for COSMO-2 simulations over the Swiss Plateau that this method overestimates h_{PBL}
11 for convective boundary layers and strongly underestimates it for stable boundary layers
12 (Collaud Coen et al., 2014).

13 Finally, the role of precipitation on FBAP concentrations is ambiguous, as already discussed
14 in section 3.1. At present, precipitation is not included as argument for the emission functions.
15 Thus, they possibly neglect a driver of the variability.

16

17 **3.4. Contribution of Fungal Spores to Near-surface Aerosol Composition**

18 For a comparison of simulated FBAP particles (in the model treated as fungal spores) to the
19 dry aerosol chemical composition, the fungal spore mass concentration is estimated from the
20 number concentration assuming monodisperse and spherical particles ($d=3\mu\text{m}$, $\rho_p = 1 \text{ g/cm}^3$;
21 section 2.1). The horizontally distributed near-surface (approximately 10 m above ground)
22 FBAP/fungal spore number concentration using F_{FBAP} is shown in Figure 10. Concentrations
23 simulated at the measurement locations are considerably lower than the high surface
24 concentrations in the southern part of the model domain.

25 The simulated mass concentrations of each chemical aerosol compound are averaged over the
26 land areas of the model domain and the time period of late August 2010 (Figure 11). The total
27 aerosol mass concentration is approximately $2.5 \mu\text{g/m}^3$. Fungal spores distribute in the
28 domain with an average number concentration of 26 L^{-1} over land. This corresponds to an
29 average mass concentration of fungal spores of $0.37 \mu\text{g/m}^3$ which accounts for 15.4% of the
30 total simulated aerosol mass. The total aerosol mass excludes mineral dust as one of the main
31 contributors to the chemical aerosol composition, which might lower the fraction of fungal

1 spore mass. A list of mass concentrations of the simulated chemical aerosol compounds,
2 including fungal spores, at the four measurement sites, is given in Table 5. The mass fraction
3 of fungal spores compared to the total aerosol simulated for these sites varies between 9% and
4 30%.

5

1 **4. Discussion and Conclusions**

2 FBAP measurements from four locations in Europe were compared with simulated
3 concentrations of fungal spores and FBAP. Fluorescent particles are often observed to be
4 most abundant in the diameter range of 2 - 4 μm (Huffman et al., 2010; Pöschl et al., 2010;
5 Huffman et al., 2012; Healy et al., 2012a; Toprak and Schnaiter, 2013; Huffman et al., 2013).
6 This diameter range for peak FBAP concentration matches closely with the modal size of
7 many species of fungal spores known to be present in the atmospheric aerosol. Contrary to
8 that, an increase in number concentration towards small particles has been reported for some
9 FBAP measurement series, although only a small fraction of FBAP could be identified as
10 bacteria cells (Gabey et al., 2011; Huffman et al., 2010). Therefore, FBAP cannot be equated
11 with fungal spores, although the concentrations of these may agree well in many cases. This
12 complicates the interpretation of the comparisons conducted in this study.

13 Comparison of simulations and measurements at four locations and the correlation of FBAP
14 concentrations to meteorological and surface conditions are expected to be most robust when
15 applying identical methods and conditions at all locations. These conditions were not fulfilled
16 in our study. On one hand, site characteristics vary between the stations, which will influence
17 the sensitivity of PBAP emission to surrounding conditions. On the other hand, the
18 measurements are made with different instruments. The measurement series at Karlsruhe,
19 Germany, are done with a WIBS-4 instrument which includes technical improvements
20 compared to the WIBS-3 used at Manchester, UK and Cork, Ireland (Gabey et al., 2010;
21 Healy et al., 2012b). At Hyytiälä, Finland, and Killarney, Ireland, the UV-APS is used to
22 determine the FBAP concentration. This variation may lead to different estimation of the
23 FBAP concentration and within this case study WIBS may report FBAP at lower
24 concentrations than UV-APS at different locations but similar meteorological conditions.

25 In this paper, fungal spore concentrations are calculated with the COSMO-ART atmospheric
26 model by using literature-based emission parameterizations which are based on the adaptation
27 of simulated global atmospheric concentration to mannitol measurements or spore colony
28 counts (Heald and Spracklen, 2009; Sesartic and Dallafior, 2011). Although mannitol
29 concentration can include contributions from other PBAP (e.g. insects, bacteria, and algae)
30 and from lower plants, the association to fungal spore concentration is reasonable (Di Filippo
31 et al., 2013). Overall, the temporal development of the literature-based simulated fungal spore
32 concentrations calculated by COSMO-ART approximately reproduces the measured FBAP

1 concentrations. Some differences between simulated fungal spore and observed FBAP
2 concentrations may be explainable by the usage of FBAP concentrations as a representative
3 for fungal spores.

4 By using a time-independent (but spatially varying) emission flux $F_{S\&D}$, every development in
5 the local temporal pattern arises from meteorological influences. A similar diurnal cycle
6 develops between simulations with constant ($F_{S\&D}$) and time-dependent ($F_{H\&S}$ and F_{FBAP})
7 fungal spore emissions, but the diurnal amplitude differs to varying extent. Therefore and
8 from a correlation analysis with the inverse of the simulated boundary layer height, a diurnal
9 cycle in the simulated fungal spore concentrations with a maximum between midnight and
10 sunrise is shown to be influenced at least partly by boundary layer compression at night.
11 However, measured FBAP concentrations are in some time periods not consistent with the
12 simulated h_{PBL} , which suggests that $N_{F,c}$ is additionally influenced e. g. by possible increases
13 in biological emission at night.

14 In this work, a new emission parameterization for FBAP particles is developed by a
15 regression analysis to observations. As was formulated by Heald and Spracklen (2009), it
16 depends on the specific humidity and the leaf area index, but is extended by temperature. The
17 resulting concentrations have on the average a smaller normalized mean bias and a slightly
18 smaller root mean square error compared to the measured FBAP concentrations than the
19 previously used fungal spore emission parameterizations, but variations in the measurements
20 are not always captured by the simulation. Thus, the correlation coefficient remains low
21 (0.43). Possible reasons include biases due to local conditions at the measurement stations,
22 biases in the input parameters and model errors related to the transport, mixing and sink
23 processes (including boundary layer turbulence and washout by precipitation). Future work
24 including a long-term analysis of FBAP concentrations and environmental conditions may
25 result in a further adjustment of the coefficients or reveal other parameters or functional
26 dependencies driving the emission. Ideally, the observations would be split into a training
27 data set and an evaluation data set, which was not possible until now due to the limited
28 amount of available observations.

29 Using the new emission parameterization on a model domain for Europe, FBAP emission
30 fluxes are extrapolated from northern parts of the domain, where UV-LIF measurements were
31 located, also to Southern Europe. There, much higher emission fluxes occur in the simulation,
32 partially caused by higher specific humidity, which is also the case for $F_{H\&S}$, as well by

1 temperature dependence in F_{FBAP} . This extrapolation is without support from local Southern
2 European measurements, however, and thus further UV-LIF measurements are recommended
3 for this region in Southern Europe where fungal spore emission fluxes are potentially larger.

4 As a result of the relatively low model horizontal resolution of 14 km, small-scale variations
5 influencing fungal spore and FBAP emission at the measurement sites may not be resolved.
6 Influences on a small scale might be due to an increased amount of fungi for the given
7 vegetation type. When taking the leaf area index as a surrogate for the vegetation type,
8 uncertainties may result from an insufficient relation to the presence of fungi or additional
9 surrounding factors favoring fungi growth. Furthermore, variations in precipitation may not
10 be captured by the model, which then may lead to biases in the fungal spore concentrations.
11 The same holds for small wind gusts and convective cells which may have a strong influence
12 on spore dispersion, but are not captured well in the model. An increase in FBAP and fungal
13 spore concentration during or shortly after rain events (Huffman et al., 2013) could not be
14 reproduced by the simulations, as this effect is not included in the emission parameterizations
15 to an adequate extent.

16 The module calculating the dispersion of FBAP/fungal spores does not include all processes
17 of aerosol dynamics and cloud physics. Of the processes not included, only breaking up of
18 spores can enhance their number concentration. Coagulation is neglected, as in most cases the
19 FBAP/fungal spore number concentration is low and, hence, their collision is highly
20 improbable. A coagulation of spores with other aerosol particles is more likely to happen, but
21 not included in the simulations. Not much is known about the role of fungal spores and other
22 biological particles in clouds and their ability to act as cloud condensation nuclei.

23 The simulations presented in this paper highlight the importance of PBAP to the composition
24 of atmospheric aerosol. Fungal spores, the focus of this paper, are among the main
25 contributors to PBAP and therefore exert significant influence on aerosol loading. In this
26 study, COSMO-ART is used to simulate all major chemical aerosol compounds except for
27 mineral dust in a domain covering Western Europe. When averaging the mass concentration
28 horizontally across the land-covered part of the model domain and over all time steps of the
29 simulation, fungal spores (assumed to be represented by FBAP) are among the major mass
30 components (Figure 11). However, the mass fraction of fungal spores might be overestimated
31 here, as another major aerosol component, mineral dust, is not included, because the domain
32 does not include any desert dust source areas. At the selected time periods, back trajectories

1 with HYSPLIT (Draxler and Rolph, 2013) and the operational dust forecast with the BSC-
2 DREAM8b model, operated by the Barcelona Supercomputing Center
3 (<http://www.bsc.es/earth-sciences/mineral-dust-forecast-system/>) suggest that transport of
4 Sahara dust to the measurement stations is low (not shown), but influences the aerosol
5 concentrations in Southern Spain. The emission from non-desert dust sources (in particular
6 agricultural areas) is strongly episodic, as it is linked not only to meteorological conditions,
7 but also to human activity (e. g. tillage operations (Funk et al., 2008; Goossens et al., 2001),
8 traffic). The magnitude of the local dust source strength is uncertain and not included in the
9 model, as no validated emission parameterization is available at present. (Beuck et al., 2011)
10 estimated that mineral dust (including both long-range transport and local sources)
11 corresponds to on average 10% of PM₁₀ concentrations in rural North-West Germany, and
12 14% of PM₁₀ concentrations in urban areas in this region.

13 The fungal spore mass concentration may reach up to 30% of simulated near-surface chemical
14 aerosol mass components in rural areas of Finland (Table 5). In comparison, ratios of PBAP
15 to total aerosol concentrations given in literature can assume similar values. The volume
16 fraction of biological particles among particles larger than 0.2 μm during one year of
17 measurements at a remote site in Siberia reaches 28% on the average and at Mainz, Germany
18 the volume fraction amounts to 22% (Matthias-Maser et al., 2000). Both of these fractions
19 agree well with simulated mass fractions of this study for comparable locations, although
20 simulated concentrations given in this study are much lower than total PBAP number
21 concentrations given in Matthias-Maser et al. (2000). In contrast, the number and mass
22 fractions in the Amazonian basin are above 80% (Pöschl et al., 2010) and therefore much
23 higher than in the urban and remote areas in this study. (Pöschl et al., 2010)

24 PBAP and especially fungal spores might account for a major part of the aerosol loading.
25 Local correlations between FBAP and ice nuclei number concentration (Tobo et al., 2013)
26 show that future model studies of PBAP impacts on clouds are needed to determine their
27 relevance to atmospheric ice nucleation.

28

29 **Acknowledgements**

30 We wish to thank Alexa Schnur for preliminary studies in connection with this paper, Max
31 Bangert for technical support, and Miriam Sinnhuber for helpful discussions on the statistical
32 analysis of our data. We would like to thank Christoph Knote and Dominik Brunner of EMPA

1 for providing the emission data of the chemical compounds. We also wish to acknowledge P.
2 Aalto, V. Hiltunen, T. Petäjä, C. Schumacher, and M. Kulmala for assistance gathering and
3 analyzing data. We acknowledge support by the Deutsche Forschungsgemeinschaft and the
4 Open Access Publishing Fund of the Karlsruhe Institute of Technology. This research was
5 funded by the Helmholtz Association through the Helmholtz Climate Initiative REKLIM and
6 the President's Initiative and Networking Fund, and by DFG through project HO 4612/1-1
7 (FOR 1525 INUIT). J. A. Huffman acknowledges internal faculty funding from the
8 University of Denver. J. A. Huffman, C. Pöhlker, and U. Pöschl acknowledge financial
9 support from the Max Planck Society (MPG), the Max Planck Graduate Center with the
10 Johannes Gutenberg University Mainz (MPGC), the LEC Geocycles Mainz, and the German
11 Research Foundation (DFG PO1013/5-1, FOR 1525 INUIT).
12

1 **References**

- 2 Ariya, P. A., Sun, J., Eltouny, N. A., Hudson, E. D., Hayes, C. T., and Kos, G.: Physical and chemical
3 characterization of bioaerosols – Implications for nucleation processes, *International Reviews in*
4 *Physical Chemistry*, 28, 1-32, 2009.
- 5 Aylor, D. E.: Settling speed of corn (*Zea mays*) pollen, *Journal of Aerosol Science*, 33, 1601-1607,
6 [http://dx.doi.org/10.1016/S0021-8502\(02\)00105-2](http://dx.doi.org/10.1016/S0021-8502(02)00105-2), 2002.
- 7 Bartholomé, E., and Belward, A. S.: GLC2000: a new approach to global land cover mapping from
8 Earth observation data, *International Journal of Remote Sensing*, 26, 1959-1977,
9 [10.1080/01431160412331291297](https://doi.org/10.1080/01431160412331291297), 2005.
- 10 Bauer, H., Schueller, E., Weinke, G., Berger, A., Hitzemberger, R., Marr, I. L., and Puxbaum, H.:
11 Significant contributions of fungal spores to the organic carbon and to the aerosol mass balance of
12 the urban atmospheric aerosol, *Atmospheric Environment*, 42, 5542-5549,
13 <http://dx.doi.org/10.1016/j.atmosenv.2008.03.019>, 2008.
- 14 Beuck, H., Quass, U., Klemm, O., and Kuhlbusch, T. A. J.: Assessment of sea salt and mineral dust
15 contributions to PM₁₀ in NW Germany using tracer models and positive matrix factorization,
16 *Atmospheric Environment*, 45, 5813-5821, <http://dx.doi.org/10.1016/j.atmosenv.2011.07.010>, 2011.
- 17 Bones, D. L., Henricksen, D. K., Mang, S. A., Gonsior, M., Bateman, A. P., Nguyen, T. B., Cooper, W. J.,
18 and Nizkorodov, S. A.: Appearance of strong absorbers and fluorophores in limonene-O₃ secondary
19 organic aerosol due to NH₄⁺-mediated chemical aging over long time scales, *Journal of Geophysical*
20 *Research: Atmospheres*, 115, D05203, [10.1029/2009jd012864](https://doi.org/10.1029/2009jd012864), 2010.
- 21 Brosseau, L. M., Vesley, D., Rice, N., Goodell, K., Nellis, M., and Hairston, P.: Differences in Detected
22 Fluorescence Among Several Bacterial Species Measured with a Direct-Reading Particle Sizer and
23 Fluorescence Detector, *Aerosol Science and Technology*, 32, 545-558, [10.1080/027868200303461](https://doi.org/10.1080/027868200303461),
24 2000.
- 25 Burch, M., and Levetin, E.: Effects of meteorological conditions on spore plumes, *International*
26 *Journal of Biometeorology*, 46, 107-117, [10.1007/s00484-002-0127-1](https://doi.org/10.1007/s00484-002-0127-1), 2002.
- 27 Burrows, S. M., Elbert, W., Lawrence, M. G., and Pöschl, U.: Bacteria in the global atmosphere – Part
28 1: Review and synthesis of literature data for different ecosystems, *Atmos. Chem. Phys.*, 9, 9263-
29 9280, [10.5194/acp-9-9263-2009](https://doi.org/10.5194/acp-9-9263-2009), 2009.
- 30 Caruana, D. J.: Detection and analysis of airborne particles of biological origin: present and future,
31 *Analyst*, 136, 4641-4652, [10.1039/c1an15506g](https://doi.org/10.1039/c1an15506g), 2011.
- 32 Christner, B. C., Morris, C. E., Foreman, C. M., Cai, R., and Sands, D. C.: Ubiquity of Biological Ice
33 Nucleators in Snowfall, *Science*, 319, 1214, [10.1126/science.1149757](https://doi.org/10.1126/science.1149757), 2008.
- 34 Collaud Coen, M., Praz, C., Haeefe, A., Ruffieux, D., Kaufmann, P., and Calpini, B.: Determination and
35 climatology of the planetary boundary layer height above the Swiss plateau by in situ and remote
36 sensing measurements as well as by the COSMO-2 model, *Atmos. Chem. Phys.*, 14, 13205-13221,
37 [10.5194/acp-14-13205-2014](https://doi.org/10.5194/acp-14-13205-2014), 2014.
- 38 Creamean, J. M., Suski, K. J., Rosenfeld, D., Cazorla, A., DeMott, P. J., Sullivan, R. C., White, A. B.,
39 Ralph, F. M., Minnis, P., Comstock, J. M., Tomlinson, J. M., and Prather, K. A.: Dust and Biological
40 Aerosols from the Sahara and Asia Influence Precipitation in the Western U.S, *Science*, 339, 1572-
41 1578, [10.1126/science.1227279](https://doi.org/10.1126/science.1227279), 2013.
- 42 DeLeon-Rodriguez, N., Latham, T. L., Rodriguez-R, L. M., Barazesh, J. M., Anderson, B. E., Beyersdorf,
43 A. J., Ziemba, L. D., Bergin, M., Nenes, A., and Konstantinidis, K. T.: Microbiome of the upper
44 troposphere: Species composition and prevalence, effects of tropical storms, and atmospheric

1 implications, Proceedings of the National Academy of Sciences, 110, 2575-2580,
2 10.1073/pnas.1212089110, 2013.

3 DeMott, P. J., and Prenni, A. J.: New Directions: Need for defining the numbers and sources of
4 biological aerosols acting as ice nuclei, Atmospheric Environment, 44, 1944-1945, 2010.

5 Després, V. R., Huffman, J. A., Burrows, S. M., Hoose, C., Safatov, A. S., Buryak, G., Fröhlich-Nowoisky,
6 J., Elbert, W., Andreae, M. O., Pöschl, U., and Jaenicke, R.: Primary biological aerosol particles in the
7 atmosphere: a review, Tellus B, 64, 15598, 10.3402/tellusb.v64i0.15598, 2012.

8 Di Filippo, P., Pomata, D., Riccardi, C., Buiarelli, F., and Perrino, C.: Fungal contribution to size-
9 segregated aerosol measured through biomarkers, Atmospheric Environment, 64, 132-140,
10 10.1016/j.atmosenv.2012.10.010, 2013.

11 Doms, G., and Schättler, U.: A Description of the Nonhydrostatic Regional COSMO-Model, Deutscher
12 Wetterdienst, Offenbach, Germany, 2002.

13 Elbert, W., Taylor, P. E., Andreae, M. O., and Pöschl, U.: Contribution of fungi to primary biogenic
14 aerosols in the atmosphere: wet and dry discharged spores, carbohydrates, and inorganic ions,
15 Atmos. Chem. Phys., 7, 4569-4588, 10.5194/acp-7-4569-2007, 2007.

16 Fang, Z. G., Ouyang, Z. Y., Zheng, H., and Wang, X. K.: Concentration and size distribution of
17 culturable airborne microorganisms in outdoor environments in Beijing, China, Aerosol Science and
18 Technology, 42, 325-334, 10.1080/02786820802068657, 2008.

19 Foot, V. E., Kaye, P. H., Stanley, W. R., Barrington, S. J., Gallagher, M., and Gabey, A.: Low-cost real-
20 time multiparameter bio-aerosol sensors, Optically Based Biological and Chemical Detection for
21 Defence IV, 7116, 71160I-71112, 2008.

22 Forster, P., Ramaswamy, V., Artaxo, P., Berntsen, T., Betts, R., Fahey, D. W., Haywood, J., Lean, J.,
23 Lowe, D. C., Myhre, G., Nganga, J., Prinn, R., Raga, G., Schulz, M., and Dorland, R. V.: Changes in
24 Atmospheric Constituents and in Radiative Forcing, in: Climate Change 2007: The Physical Science
25 Basis. Contribution of Working Group I to the Fourth Assessment Report of the Intergovernmental
26 Panel on Climate Change, edited by: Solomon, S., Qin, D., Manning, M., Chen, Z., Marquis, M., Averyt,
27 K. B., M.Tignor, and (eds.), H. L. M., Cambridge University Press, Cambridge, United Kingdom and
28 New York, NY, USA, 2007.

29 Fountoukis, C., and Nenes, A.: ISORROPIA II: a computationally efficient thermodynamic equilibrium
30 model for K^+ - Ca^{2+} - Mg^{2+} - NH_4^+ - Na^+ - SO_4^{2-} - NO_3^- - Cl^- - H_2O aerosols, Atmos. Chem. Phys., 7, 4639-
31 4659, 10.5194/acp-7-4639-2007, 2007.

32 Fröhlich-Nowoisky, J., Burrows, S. M., Xie, Z., Engling, G., Solomon, P. A., Fraser, M. P., Mayol-
33 Bracero, O. L., Artaxo, P., Begerow, D., Conrad, R., Andreae, M. O., Després, V. R., and Pöschl, U.:
34 Biogeography in the air: fungal diversity over land and oceans, Biogeosciences, 9, 1125-1136,
35 10.5194/bg-9-1125-2012, 2012.

36 Funk, R., Reuter, H. I., Hoffmann, C., Engel, W., and Öttl, D.: Effect of moisture on fine dust emission
37 from tillage operations on agricultural soils, Earth Surface Processes and Landforms, 33, 1851-1863,
38 10.1002/esp.1737, 2008.

39 Gabey, A. M., Gallagher, M. W., Whitehead, J., Dorsey, J. R., Kaye, P. H., and Stanley, W. R.:
40 Measurements and comparison of primary biological aerosol above and below a tropical forest
41 canopy using a dual channel fluorescence spectrometer, Atmospheric Chemistry and Physics, 10,
42 4453-4466, 10.5194/acp-10-4453-2010, 2010.

43 Gabey, A. M., Stanley, W. R., Gallagher, M. W., and Kaye, P. H.: The fluorescence properties of
44 aerosol larger than 0.8 μm in urban and tropical rainforest locations, Atmos. Chem. Phys., 11, 5491-
45 5504, 10.5194/acp-11-5491-2011, 2011.

- 1 Gabey, A. M., Vaitilingom, M., Freney, E., Boulon, J., Sellegri, K., Gallagher, M. W., Crawford, I. P.,
2 Robinson, N. H., Stanley, W. R., and Kaye, P. H.: Observations of fluorescent and biological aerosol at
3 a high-altitude site in central France, *Atmos. Chem. Phys.*, 13, 7415-7428, 10.5194/acp-13-7415-
4 2013, 2013.
- 5 Goossens, D., Gross, J., and Spaan, W.: Aeolian dust dynamics in agricultural land areas in Lower
6 Saxony, Germany, *Earth Surface Processes and Landforms*, 26, 701-720, 10.1002/esp.216, 2001.
- 7 Graham, B., Guyon, P., Maenhaut, W., Taylor, P. E., Ebert, M., Matthias-Maser, S., Mayol-Bracero, O.
8 L., Godoi, R. H. M., Artaxo, P., Meixner, F. X., Moura, M. A. L., Rocha, C. H. E. D. A., Grieken, R. V.,
9 Glovsky, M. M., Flagan, R. C., and Andreae, M. O.: Composition and diurnal variability of the natural
10 Amazonian aerosol, *Journal of Geophysical Research: Atmospheres*, 108, 4765,
11 10.1029/2003jd004049, 2003.
- 12 Gregory, P. H.: *The microbiology of the atmosphere*, Plant Science Monographs, edited by: Polunin,
13 N., Leonard Hill, London, 1961.
- 14 Haga, D. I., Iannone, R., Wheeler, M. J., Mason, R., Polishchuk, E. A., Fetch, T., van der Kamp, B. J.,
15 McKendry, I. G., and Bertram, A. K.: Ice nucleation properties of rust and bunt fungal spores and their
16 transport to high altitudes where they can cause heterogeneous freezing, *Journal of Geophysical
17 Research: Atmospheres*, n/a-n/a, 10.1002/jgrd.50556, 2013.
- 18 Hairston, P. P., Ho, J., and Quant, F. R.: Design of an instrument for real-time detection of bioaerosols
19 using simultaneous measurement of particle aerodynamic size and intrinsic fluorescence, *J Aerosol
20 Sci*, 28, 471-482, 1997.
- 21 Hameed, A. A. A., and Khodr, M. I.: Suspended particulates and bioaerosols emitted from an
22 agricultural non-point source, *J. Environ. Monit.*, 3, 206-209, 2001.
- 23 Heald, C. L., and Spracklen, D. V.: Atmospheric budget of primary biological aerosol particles from
24 fungal spores, *Geophys. Res. Lett.*, 36, L09806, 10.1029/2009gl037493, 2009.
- 25 Healy, D. A., O'Connor, D. J., Burke, A. M., and Sodeau, J. R.: A laboratory assessment of the
26 Waveband Integrated Bioaerosol Sensor (WIBS-4) using individual samples of pollen and fungal spore
27 material, *Atmospheric Environment*, 60, 534-543,
28 <http://dx.doi.org/10.1016/j.atmosenv.2012.06.052>, 2012a.
- 29 Healy, D. A., O'Connor, D. J., and Sodeau, J. R.: Measurement of the particle counting efficiency of
30 the "Waveband Integrated Bioaerosol Sensor" model number 4 (WIBS-4), *Journal of Aerosol Science*,
31 47, 94-99, <http://dx.doi.org/10.1016/j.jaerosci.2012.01.003>, 2012b.
- 32 Healy, D. A., Huffman, J. A., O'Connor, D. J., Pöhlker, C., Pöschl, U., and Sodeau, J. R.: Ambient
33 measurements of biological aerosol particles near Killarney, Ireland: a comparison between real-time
34 fluorescence and microscopy techniques, *Atmos. Chem. Phys.*, 14, 8055-8069, 10.5194/acp-14-8055-
35 2014, 2014.
- 36 Helbig, N., Vogel, B., Vogel, H., and Fiedler, F.: Numerical modelling of pollen dispersion on the
37 regional scale, *Aerobiologia*, 20, 3-19, 10.1023/b:aero.0000022984.51588.30, 2004.
- 38 Hoose, C., Kristjánsson, J. E., and Burrows, S. M.: How important is biological ice nucleation in clouds
39 on a global scale?, *Environmental Research Letters*, 5, 024009, 2010a.
- 40 Hoose, C., Kristjánsson, J. E., Chen, J.-P., and Hazra, A.: A Classical-Theory-Based Parameterization of
41 Heterogeneous Ice Nucleation by Mineral Dust, Soot, and Biological Particles in a Global Climate
42 Model, *Journal of the Atmospheric Sciences*, 67, 2483-2503, 10.1175/2010jas3425.1, 2010b.

- 1 Hoose, C., and Möhler, O.: Heterogeneous ice nucleation on atmospheric aerosols: a review of
2 results from laboratory experiments, *Atmos. Chem. Phys.*, 12, 9817-9854, 10.5194/acp-12-9817-
3 2012, 2012.
- 4 Huffman, J. A., Treutlein, B., and Pöschl, U.: Fluorescent biological aerosol particle concentrations
5 and size distributions measured with an Ultraviolet Aerodynamic Particle Sizer (UV-APS) in Central
6 Europe, *Atmospheric Chemistry and Physics*, 10, 3215-3233, 2010.
- 7 Huffman, J. A., Sinha, B., Garland, R. M., Snee-Pollmann, A., Gunthe, S. S., Artaxo, P., Martin, S. T.,
8 Andreae, M. O., and Pöschl, U.: Size distributions and temporal variations of biological aerosol
9 particles in the Amazon rainforest characterized by microscopy and real-time UV-APS fluorescence
10 techniques during AMAZE-08, *Atmos. Chem. Phys.*, 12, 11997-12019, 10.5194/acp-12-11997-2012,
11 2012.
- 12 Huffman, J. A., Prenni, A. J., DeMott, P. J., Pöhlker, C., Mason, R. H., Robinson, N. H., Fröhlich-
13 Nowoisky, J., Tobo, Y., Després, V. R., Garcia, E., Gochis, D. J., Harris, E., Müller-Germann, I., Ruzene,
14 C., Schmer, B., Sinha, B., Day, D. A., Andreae, M. O., Jimenez, J. L., Gallagher, M., Kreidenweis, S. M.,
15 Bertram, A. K., and Pöschl, U.: High concentrations of biological aerosol particles and ice nuclei
16 during and after rain, *Atmos. Chem. Phys.*, 13, 6151-6164, 10.5194/acp-13-6151-2013, 2013.
- 17 Jacobson, M. Z., and Streets, D. G.: Influence of future anthropogenic emissions on climate, natural
18 emissions, and air quality, *Journal of Geophysical Research: Atmospheres*, 114, D08118,
19 10.1029/2008jd011476, 2009.
- 20 Jaenicke, R.: Über die Dynamik atmosphärischer Aitkenteilchen, in: *Berichte der Bunsengesellschaft
21 für physikalische Chemie*, 11, Wiley-VCH Verlag GmbH & Co. KGaA, 1198-1202, 1978.
- 22 Jaenicke, R., Matthias-Maser, S., and Gruber, S.: Omnipresence of biological material in the
23 atmosphere, *Environmental Chemistry*, 4, 217-220, <http://dx.doi.org/10.1071/EN07021>, 2007.
- 24 Jones, A. M., and Harrison, R. M.: The effects of meteorological factors on atmospheric bioaerosol
25 concentrations--a review, *Science of The Total Environment*, 326, 151-180,
26 10.1016/j.scitotenv.2003.11.021, 2004.
- 27 Kaye, P., Stanley, W. R., Hirst, E., Foot, E. V., Baxter, K. L., and Barrington, S. J.: Single particle
28 multichannel bio-aerosol fluorescence sensor, *Opt. Express*, 13, 3583-3593,
29 10.1364/opex.13.003583, 2005.
- 30 Knote, C., Brunner, D., Vogel, H., Allan, J., Asmi, A., Äijälä, M., Carbone, S., van der Gon, H. D.,
31 Jimenez, J. L., Kiendler-Scharr, A., Mohr, C., Poulain, L., Prévôt, A. S. H., Swietlicki, E., and Vogel, B.:
32 Towards an online-coupled chemistry-climate model: evaluation of trace gases and aerosols in
33 COSMO-ART, *Geosci. Model Dev.*, 4, 1077-1102, 10.5194/gmd-4-1077-2011, 2011.
- 34 Knyazikhin, Y., Martonchik, J. V., Myneni, R. B., Diner, D. J., and Running, S. W.: Synergistic algorithm
35 for estimating vegetation canopy leaf area index and fraction of absorbed photosynthetically active
36 radiation from MODIS and MISR data, *Journal of Geophysical Research: Atmospheres*, 103, 32257-
37 32275, 10.1029/98JD02462, 1998.
- 38 Kuenen, J., Denier van der Gon, H., Visschedijk, A., van der Brugh, H., and Gijlswijk, R.: MACC
39 European emission inventory for the years 2003–2007, TNO, Utrecht, Netherlands, TNO-060-UT-
40 2011-00588, 49, 2011.
- 41 Lee, H. J., Laskin, A., Laskin, J., and Nizkorodov, S. A.: Excitation–Emission Spectra and Fluorescence
42 Quantum Yields for Fresh and Aged Biogenic Secondary Organic Aerosols, *Environmental Science &
43 Technology*, 47, 5763-5770, 10.1021/es400644c, 2013.
- 44 Lin, W.-H., and Li, C.-S.: Size Characteristics of Fungus Allergens in the Subtropical Climate, *Aerosol
45 Science and Technology*, 25, 93-100, 10.1080/02786829608965382, 1996.

1 Lundgren, K., Vogel, B., Vogel, H., and Kottmeier, C.: Direct radiative effects of sea salt for the
2 Mediterranean region under conditions of low to moderate wind speeds, *Journal of Geophysical*
3 *Research: Atmospheres*, 118, 1906-1923, 10.1029/2012jd018629, 2013.

4 Mahowald, N., Jickells, T. D., Baker, A. R., Artaxo, P., Benitez-Nelson, C. R., Bergametti, G., Bond, T. C.,
5 Chen, Y., Cohen, D. D., Herut, B., Kubilay, N., Losno, R., Luo, C., Maenhaut, W., McGee, K. A., Okin, G.
6 S., Siefert, R. L., and Tsukuda, S.: Global distribution of atmospheric phosphorus sources,
7 concentrations and deposition rates, and anthropogenic impacts, *Global Biogeochemical Cycles*, 22,
8 GB4026, 10.1029/2008gb003240, 2008.

9 Martin, S. T., Andreae, M. O., Artaxo, P., Baumgardner, D., Chen, Q., Goldstein, A. H., Guenther, A.,
10 Heald, C. L., Mayol-Bracero, O. L., McMurry, P. H., Pauliquevis, T., Pöschl, U., Prather, K. A., Roberts,
11 G. C., Saleska, S. R., Silva Dias, M. A., Spracklen, D. V., Swietlicki, E., and Trebs, I.: Sources and
12 properties of Amazonian aerosol particles, *Reviews of Geophysics*, 48, RG2002,
13 10.1029/2008rg000280, 2010.

14 Matthias-Maser, S., Obolkin, V., Khodzer, T., and Jaenicke, R.: Seasonal variation of primary biological
15 aerosol particles in the remote continental region of Lake Baikal/Siberia, *Atmospheric Environment*,
16 34, 3805-3811, 10.1016/s1352-2310(00)00139-4, 2000.

17 Morris, C. E., Georgakopoulos, D. G., and Sands, D. C.: Ice nucleation active bacteria and their
18 potential role in precipitation, *J. Phys. IV France*, 121, 87-103, 2004.

19 Morris, C. E., Sands, D. C., Glaux, C., Samsatly, J., Asaad, S., Moukahel, A. R., Gonçalves, F. L. T., and
20 Bigg, E. K.: Urediospores of rust fungi are ice nucleation active at > -10 °C and harbor ice nucleation
21 active bacteria, *Atmos. Chem. Phys.*, 13, 4223-4233, 10.5194/acp-13-4223-2013, 2013.

22 Murray, B. J., O'Sullivan, D., Atkinson, J. D., and Webb, M. E.: Ice nucleation by particles immersed in
23 supercooled cloud droplets, *Chemical Society Reviews*, 41, 6519-6554, 2012.

24 O'Connor, D. J., Healy, D. A., Hellebust, S., Buters, J. T. M., and Sodeau, J. R.: Using the WIBS-4
25 (Waveband Integrated Bioaerosol Sensor) technique for the on-line detection of pollen grains,
26 *Aerosol Science and Technology*, 48, 10.1080/02786826.2013.872768, 2014.

27 Olson, D. M., Dinerstein, E., Wikramanayake, E. D., Burgess, N. D., Powell, G. V. N., Underwood, E. C.,
28 D'Amico, J. A., Itoua, I., Strand, H. E., Morrison, J. C., Loucks, C. J., Allnutt, T. F., Ricketts, T. H., Kura,
29 Y., Lamoreux, J. F., Wettengel, W. W., Hedao, P., and Kassem, K. R.: Terrestrial Ecoregions of the
30 World: A New Map of Life on Earth, *BioScience*, 51, 933-938, 10.1641/0006-
31 3568(2001)051[0933:teotwa]2.0.co;2, 2001.

32 Pan, Y.-I., Holler, S., Chang, R. K., Hill, S. C., Pinnick, R. G., Niles, S., and Bottiger, J. R.: Single-shot
33 fluorescence spectra of individual micrometer-sized bioaerosols illuminated by a 351- or a 266-nm
34 ultraviolet laser, *Opt. Lett.*, 24, 116-118, 10.1364/ol.24.000116, 1999.

35 Penner, J. E.: Carbonaceous aerosols influencing atmospheric radiation: black and organic carbon, in:
36 *Aerosol Forcing of Climate*, edited by: Charlson, R. J. a. H., J., John Wiley and Sons, Chichester, 91 -
37 108, 1995.

38 Petters, M. D., and Kreidenweis, S. M.: A single parameter representation of hygroscopic growth and
39 cloud condensation nucleus activity, *Atmos. Chem. Phys.*, 7, 1961-1971, 10.5194/acp-7-1961-2007,
40 2007.

41 Pöhlker, C., Huffman, J. A., and Pöschl, U.: Autofluorescence of atmospheric bioaerosols – fluorescent
42 biomolecules and potential interferences, *Atmos. Meas. Tech.*, 5, 37-71, 10.5194/amt-5-37-2012,
43 2012.

- 1 Pöhlker, C., Huffman, J. A., Förster, J. D., and Pöschl, U.: Autofluorescence of atmospheric
2 bioaerosols: spectral fingerprints and taxonomic trends of pollen, *Atmos. Meas. Tech.*, 6, 3369-3392,
3 10.5194/amt-6-3369-2013, 2013.
- 4 Pope, F. D.: Pollen grains are efficient cloud condensation nuclei, *Environmental Research Letters*, 5,
5 044015, 2010.
- 6 Pöschl, U., Martin, S. T., Sinha, B., Chen, Q., Gunthe, S. S., Huffman, J. A., Borrmann, S., Farmer, D. K.,
7 Garland, R. M., Helas, G., Jimenez, J. L., King, S. M., Manzi, A., Mikhailov, E., Pauliquevis, T., Petters,
8 M. D., Prenni, A. J., Roldin, P., Rose, D., Schneider, J., Su, H., Zorn, S. R., Artaxo, P., and Andreae, M.
9 O.: Rainforest Aerosols as Biogenic Nuclei of Clouds and Precipitation in the Amazon, *Science*, 329,
10 1513-1516, 10.1126/science.1191056, 2010.
- 11 Prenni, A. J., Petters, M. D., Kreidenweis, S. M., Heald, C. L., Martin, S. T., Artaxo, P., Garland, R. M.,
12 Wollny, A. G., and Pöschl, U.: Relative roles of biogenic emissions and Saharan dust as ice nuclei in
13 the Amazon basin, *Nature Geosci.*, 2, 402-405, 2009.
- 14 Prenni, A. J., Tobo, Y., Garcia, E., DeMott, P. J., Huffman, J. A., McCluskey, C. S., Kreidenweis, S. M.,
15 Prenni, J. E., Pöhlker, C., and Pöschl, U.: The impact of rain on ice nuclei populations at a forested site
16 in Colorado, *Geophysical Research Letters*, 40, 227-231, 10.1029/2012gl053953, 2013.
- 17 Ramankutty, N., Evan, A. T., Monfreda, C., and Foley, J. A.: Farming the planet: 1. Geographic
18 distribution of global agricultural lands in the year 2000, *Global Biogeochem. Cycles*, 22, GB1003,
19 10.1029/2007gb002952, 2008.
- 20 Reponen, T., Grinshpun, S. A., Conwell, K. L., Wiest, J., and Anderson, M.: Aerodynamic versus
21 physical size of spores: Measurement and implication for respiratory deposition, *Grana*, 40, 119-125,
22 10.1080/00173130152625851, 2001.
- 23 Rinke, R.: Parametrisierung des Auswaschens von Aerosolpartikeln durch Niederschlag, Ph.D., Inst.
24 für Meteorol. und Klimaforsch., Univ. Karlsruhe (TH), Karlsruhe, Germany, 2008.
- 25 Robinson, N. H., Allan, J. D., Huffman, J. A., Kaye, P. H., Foot, V. E., and Gallagher, M.: Cluster analysis
26 of WBS single-particle bioaerosol data, *Atmos. Meas. Tech.*, 6, 337-347, 10.5194/amt-6-337-2013,
27 2013.
- 28 Saari, S. E., Putkiranta, M. J., and Keskinen, J.: Fluorescence spectroscopy of atmospherically relevant
29 bacterial and fungal spores and potential interferences, *Atmospheric Environment*, 71, 202-209,
30 <http://dx.doi.org/10.1016/j.atmosenv.2013.02.023>, 2013.
- 31 Schell, B., Ackermann, I. J., Hass, H., Binkowski, F. S., and Ebel, A.: Modeling the formation of
32 secondary organic aerosol within a comprehensive air quality model system, *Journal of Geophysical
33 Research: Atmospheres*, 106, 28275-28293, 10.1029/2001jd000384, 2001.
- 34 Schumacher, C. J., Pöhlker, C., Aalto, P., Hiltunen, V., Petäjä, T., Kulmala, M., Pöschl, U., and Huffman,
35 J. A.: Seasonal cycles of fluorescent biological aerosol particles in boreal and semi-arid forests of
36 Finland and Colorado, *Atmos. Chem. Phys.*, 13, 11987-12001, 10.5194/acp-13-11987-2013, 2013.
- 37 Seinfeld, J. H., and Pandis, S. N.: *Atmospheric Chemistry and Physics - From Air Pollution to Climate
38 Change (2nd Edition)*, John Wiley & Sons, Hoboken, New Jersey, USA, 2006.
- 39 Sesartic, A., and Dallafior, T. N.: Global fungal spore emissions, review and synthesis of literature
40 data, *Biogeosciences*, 8, 1181-1192, 10.5194/bg-8-1181-2011, 2011.
- 41 Sesartic, A., Lohmann, U., and Storelvmo, T.: Bacteria in the ECHAM5-HAM global climate model,
42 *Atmos. Chem. Phys.*, 12, 8645-8661, 10.5194/acp-12-8645-2012, 2012.
- 43 Shaffer, B. T., and Lighthart, B.: Survey of Culturable Airborne Bacteria at Four Diverse Locations in
44 Oregon: Urban, Rural, Forest, and Coastal, *Microbial Ecology*, 34, 167-177, 10.2307/4251522, 1997.

1 Spracklen, D. V., and Heald, C. L.: The contribution of fungal spores and bacteria to regional and
2 global aerosol number and ice nucleation immersion freezing rates, *Atmos. Chem. Phys. Discuss.*, 13,
3 32459-32481, 10.5194/acpd-13-32459-2013, 2013.

4 Szintai, B., and Kaufmann, P.: TKE as a Measure of Turbulence, *COSMO Newsletter*, 8, 2-10, 2008.

5 Tobo, Y., Prenni, A. J., DeMott, P. J., Huffman, J. A., McCluskey, C. S., Tian, G., Pöhlker, C., Pöschl, U.,
6 and Kreidenweis, S. M.: Biological aerosol particles as a key determinant of ice nuclei populations in a
7 forest ecosystem, *Journal of Geophysical Research: Atmospheres*, n/a-n/a, 10.1002/jgrd.50801,
8 2013.

9 Toprak, E., and Schnaiter, M.: Fluorescent biological aerosol particles measured with the Waveband
10 Integrated Bioaerosol Sensor WIBS-4: laboratory tests combined with a one year field study, *Atmos.*
11 *Chem. Phys.*, 13, 225-243, 10.5194/acp-13-225-2013, 2013.

12 Trail, F., Gaffoor, I., and Vogel, S.: Ejection mechanics and trajectory of the ascospores of *Gibberella*
13 *zeae* (anamorph *Fuarium graminearum*), *Fungal Genetics and Biology*, 42, 528-533,
14 10.1016/j.fgb.2005.03.008, 2005.

15 Vogel, B., Vogel, H., Bäumer, D., Bangert, M., Lundgren, K., Rinke, R., and Stanelle, T.: The
16 comprehensive model system COSMO-ART – radiative impact of aerosol on the state of the
17 atmosphere on the regional scale, *Atmos. Chem. Phys.*, 9, 14483-14528, 10.5194/acpd-9-14483-
18 2009, 2009.

19 Vogel, H., Pauling, A., and Vogel, B.: Numerical simulation of birch pollen dispersion with an
20 operational weather forecast system, *International Journal of Biometeorology*, 52, 805-814,
21 10.1007/s00484-008-0174-3, 2008.

22 Winiwarter, W., Bauer, H., Caseiro, A., and Puxbaum, H.: Quantifying emissions of primary biological
23 aerosol particle mass in Europe, *Atmospheric Environment*, 43, 1403-1409,
24 <http://dx.doi.org/10.1016/j.atmosenv.2008.01.037>, 2009.

25 Yamamoto, N., Bibby, K., Qian, J., Hospodsky, D., Rismani-Yazdi, H., Nazaroff, W. W., and Peccia, J.:
26 Particle-size distributions and seasonal diversity of allergenic and pathogenic fungi in outdoor air,
27 *ISME J*, 6, 1801-1811, 2012.

28

29

1 Table 1. Overview of the measurement sites, including their geographical location and the types of instrument
 2 used (d_p corresponds to the optical particle diameter and d_a to the aerodynamic particle diameter). The sections
 3 below show the simulation periods and the availability of data at this site (filled dot). Mean values for the
 4 simulated meteorological and surface conditions used for the new emission parameterization (section 3.2) at the
 5 measurement site during the corresponding time periods are added to each section.

location	Karlsruhe, Germany	Hyytiälä, Finland	Manchester, UK	Killarney, Ireland
coordinates	49° 5' 43.6" N 8° 25' 45.0" E	61° 50' 41.0" N 24° 17' 17.4" E	53° 27' 57.0" N 2° 13' 56.0" W	52° 3' 28.0" N 9° 30' 16.4" W
altitude	111 m a.s.l.	152 m a.s.l.	45 m a.s.l.	34 m a.s.l.
instrument	WIBS-4	UV-APS	WIBS-3	UV-APS
size range	$0.8 \leq d_p \leq 16 \mu\text{m}$	$1 < d_a \leq 20 \mu\text{m}$	$0.8 \leq d_p \leq 20 \mu\text{m}$	$1 < d_a \leq 20 \mu\text{m}$
22 July 2010 - 28 July 2010	●	●	○	○
LAI (m^2/m^2)	3.18	3.72	-	-
mean T ($^{\circ}\text{C}$)	17.3	16.2	-	-
mean q_v (kg/kg)	0.0088	0.0108	-	-
26 August 2010 - 01 September 2010	●	●	●	●
LAI (m^2/m^2)	2.94	3.4	2.87	2.06
mean T ($^{\circ}\text{C}$)	16.6	8.5	11.6	11.1
mean q_v (kg/kg)	0.0099	0.0067	0.0073	0.0072
11 October 2010 - 21 October 2010	●	●	○	○
LAI (m^2/m^2)	1.49	1.27	-	-
mean T ($^{\circ}\text{C}$)	6.5	-0.6	-	-
mean q_v (kg/kg)	0.0055	0.0034	-	-

6

7

1 Table 2. Correlation coefficient (R), root mean square error (RMSE) and normalized mean bias (NMB) for
 2 correlations between simulated fungal spore/FBAP and measured FBAP concentrations at different locations and
 3 three different time periods.

	N _{H&S}			N _{S&D}			N _{FBAP}			Confidence intervals for R	
	R	RMSE [L ⁻¹]	NMB [%]	R	RMSE [L ⁻¹]	NMB [%]	R	RMSE [L ⁻¹]	NMB [%]	95%	99%
Karlsruhe, Jul10	0.07	45	-58	0.11	48	-66	0.07	38	-32	±0.17	±0.22
Karlsruhe, Aug10	0.11	25	-36	-0.07	28	-40	0.11	30	1.4	±0.16	±0.20
Karlsruhe, Oct10	-0.11	22	-64	0.01	21	20	-0.17	17	-35	±0.18	±0.23
Hyytiälä, Jul10	0.57	17	3.2	0.58	24	-67	0.57	23	51	±0.11	±0.15
Hyytiälä, Aug10	0.04	20	-62	0.19	22	-76	0.00	18	-46	±0.16	±0.21
Hyytiälä, Oct10	0.01	4.7	-58	-0.10	5.1	35	0.23	4.6	-59	±0.17	±0.23
Manchester, Aug10	0.68	15	2.7	0.65	19	38	0.66	22	63	±0.09	±0.12
Killarney, Aug10	0.49	6.6	84	0.32	15	200	0.45	15	214	±0.13	±0.17
all	0.428	26.2	-44.04	-0.05	25.6	-28.74	0.433	23.2	-0.43	±0.05	±0.06

4

1 Table 3. Correlation coefficient (R) and confidence intervals for correlations between observed FBAP
 2 concentrations and the inverse boundary layer height at different locations and three different time periods.

	R	95% confidence interval	99% confidence interval
Karlsruhe, Jul10	0.11	±0.16	±0.21
Karlsruhe, Aug10	-0.03	±0.16	±0.21
Karlsruhe, Oct10	-0.12	±0.15	±0.19
Hyytiälä, Jul10	0.35	±0.15	±0.19
Hyytiälä, Aug10	0.32	±0.14	±0.18
Hyytiälä, Oct10	-0.20	±0.18	±0.23
Manchester, Aug10	0.52	±0.12	±0.15
Killarney, Aug10	0.29	±0.14	±0.19
all	0.11	±0.06	±0.07
all, without h<10 m	0.18	±0.06	±0.07

3

4

1 Table 4. Leaf area index (m^2/m^2) from the climatological GLC2000 dataset as used in the simulations compared
 2 to the nearest neighbor pixel of the 8-day, 1 km resolution MODIS LAI and to an average of the 1 km resolution
 3 MODIS LAI over a 20x20 km area centered on the station gridpoint. In addition, the standard deviation within
 4 that 20x20 km area is given. For the Manchester nearest neighbor 1 km gridpoint, no data are available for the
 5 given time period.

		Karlsruhe	Hyytiälä	Manchester	Killarney
22 Jul–28 Jul 2010	GLC2000	3.18	3.72	-	-
	MODIS 1 km	2.30	4.80	-	-
	MODIS 20 km average	2.70	3.77	-	-
	MODIS 20 km std dev	1.64	1.34	-	-
26 Aug–1 Sep 2010	GLC2000	2.94	3.40	2.87	2.06
	MODIS 1 km	3.46	1.59	n.d.	3.20
	MODIS 20 km average	2.62	1.65	1.28	3.15
	MODIS 20 km std dev	1.48	1.10	0.66	1.97
11 Oct–21 Oct 2010	GLC2000	1.49	1.27	-	-
	MODIS 1 km	1.62	0.80	-	-
	MODIS 20km average	1.41	1.32	-	-
	MODIS 20 km std dev	0.93	0.96	-	-

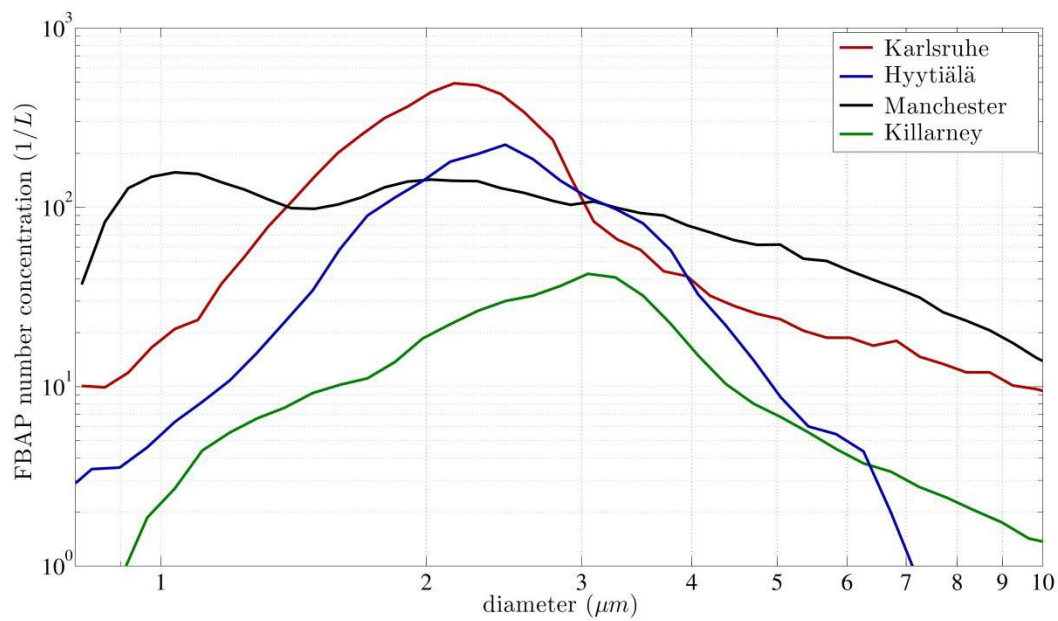
6

1 Table 5. Simulated aerosol mass concentrations for aerosol chemical components, including fungal spores, in
 2 $\mu\text{g}/\text{m}^3$ at the measuring sites as averages over the time period during August 2010

Particle Mass ($\mu\text{g}/\text{m}^3$)	Karlsruhe, Germany	Hyytiälä, Finland	Manchester, UK	Killarney, Ireland
fungal spores	0.41	0.20	0.35	0.28
sea salt	0.44	0.01	1.62	1.11
soot	0.19	0.06	0.42	0.04
SO_4^{2-}	0.18	0.01	0.11	0.05
NH_4^+	0.44	0.01	0.14	0.07
NO_3^-	1.29	0.01	0.34	0.18
SOA	0.41	0.24	0.14	0.04
aPOA	0.67	0.13	0.85	0.11

3
 4
 5

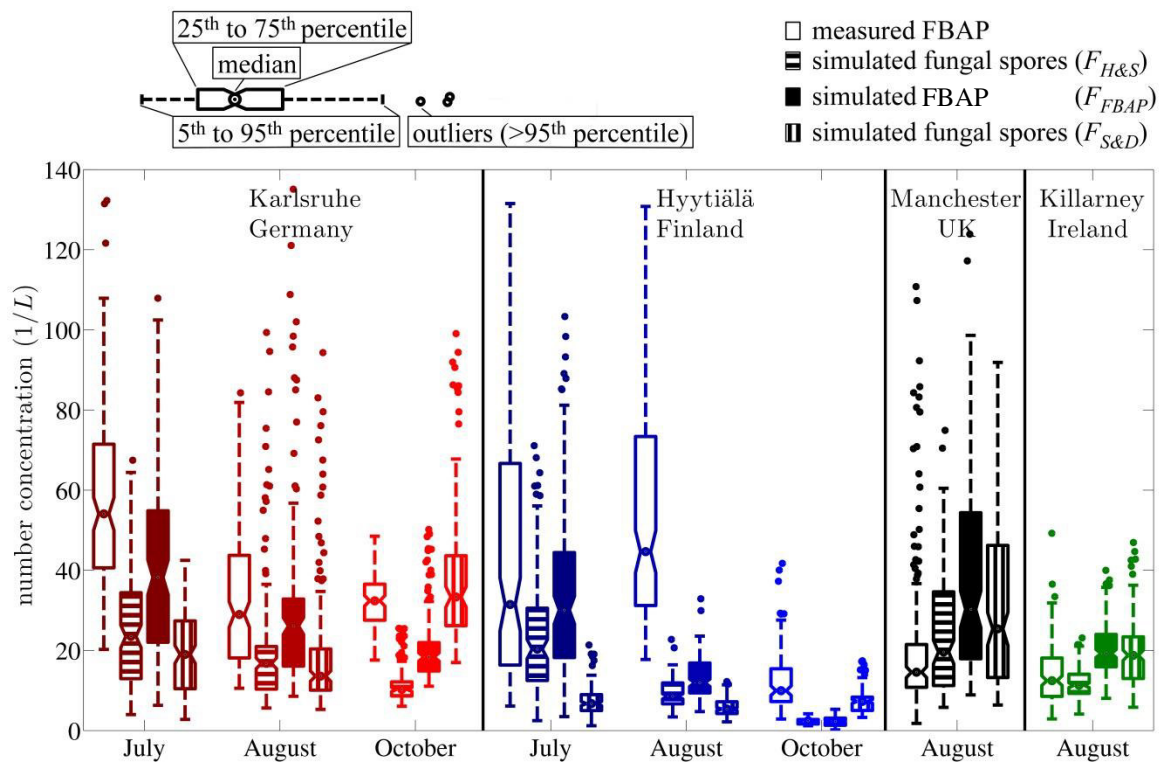
1



2

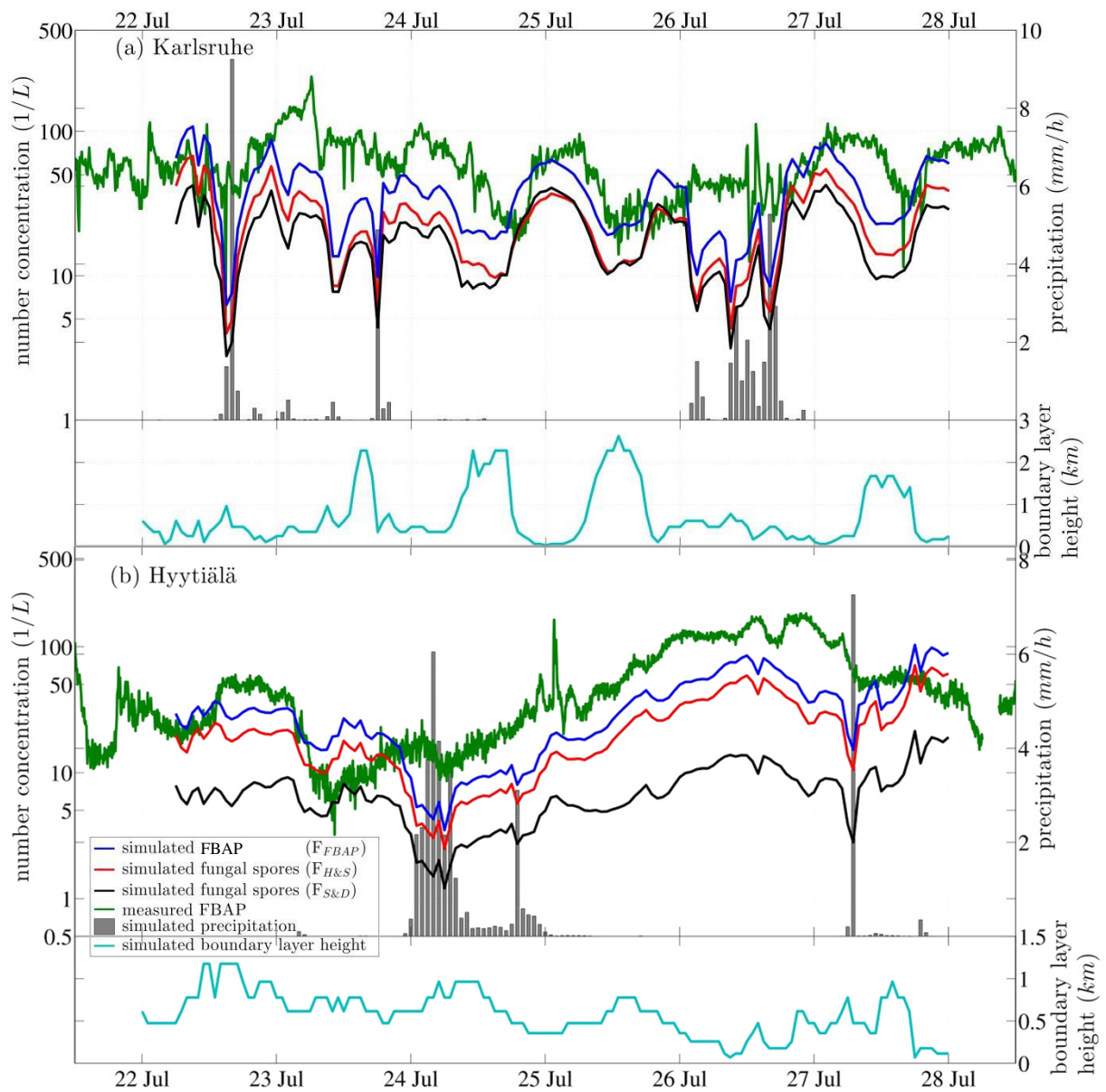
3 Figure 1. Average FBAP size distributions derived from UV-LIF measurements during case studies in August
4 2010 at Karlsruhe (Germany) with WIBS-4, Hyytiälä (Finland) with UV-APS, Manchester (UK) with WIBS-3,
5 and Killarney (Ireland) with UV-APS.

6



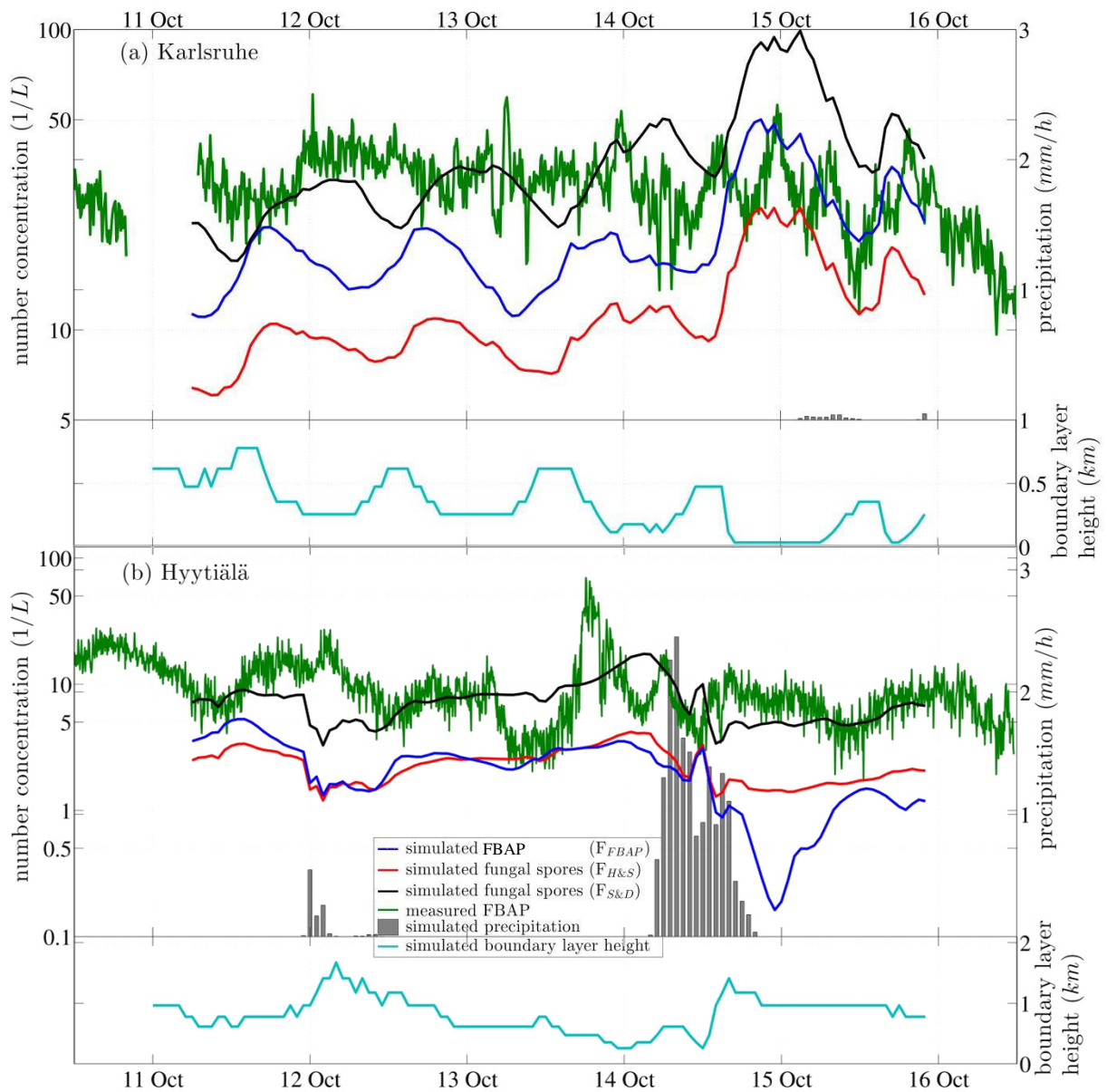
1
 2 Figure 2. Box-whisker plots for all case studies of: measured hourly FBAP concentration (open boxes),
 3 simulated fungal spore concentration with three different emission parameterizations: $F_{H\&S}$ from Heald and
 4 Spracklen (2009, horizontally hatched boxes); F_{FBAP} from this study (filled boxes); $F_{S\&D}$ from Sesartic and
 5 Dallafior (2011, vertically hatched boxes). The central mark of each box shows the median, its edges the 25th and
 6 75th percentiles, and whiskers show 5th and 95th percentiles. Dots above whisker show outliers (>95th percentile).

7



1
 2 Figure 3. Time series of measured FBAP and simulated fungal spore/FBAP number concentrations in 1/L
 3 together with simulated precipitation in mm/h (right axis) and simulated boundary layer height in km (right axis)
 4 during the case study from 22 July to 28 July 2010 at (a) Karlsruhe, Germany and (b) Hyytiälä, Finland.
 5 Simulations were performed with three different emission parameterizations: $F_{H\&S}$ from Heald and Spracklen
 6 (2009); $F_{S\&D}$ from Sesartic and Dallafior (2011); F_{FBAP} from this study.

7

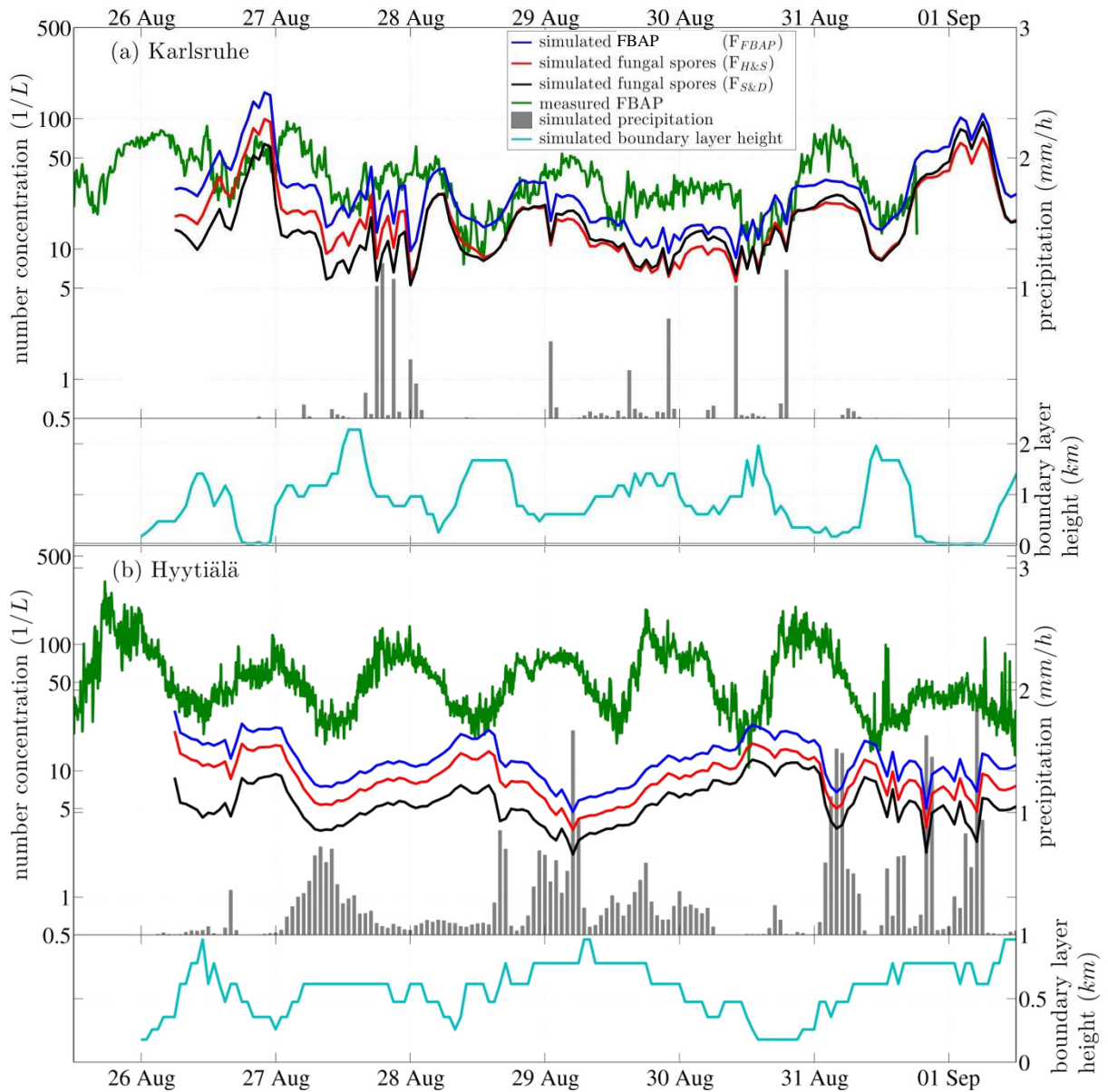


1

2 Figure 4. Time series of measured FBAP and simulated fungal spore/FBAP number concentrations in $1/L$
 3 together with simulated precipitation in mm/h (right axis) and simulated boundary layer height in km (right axis)
 4 during the case study from 11 October 2010 to 21 October 2010 at (a) Karlsruhe, Germany and (b) Hyytiälä,
 5 Finland. Simulations were performed with three different emission parameterizations: $F_{H\&S}$ from Heald and
 6 Spracklen (2009); $F_{S\&D}$ from Sesartic and Dallafior (2011); F_{FBAP} from this study.

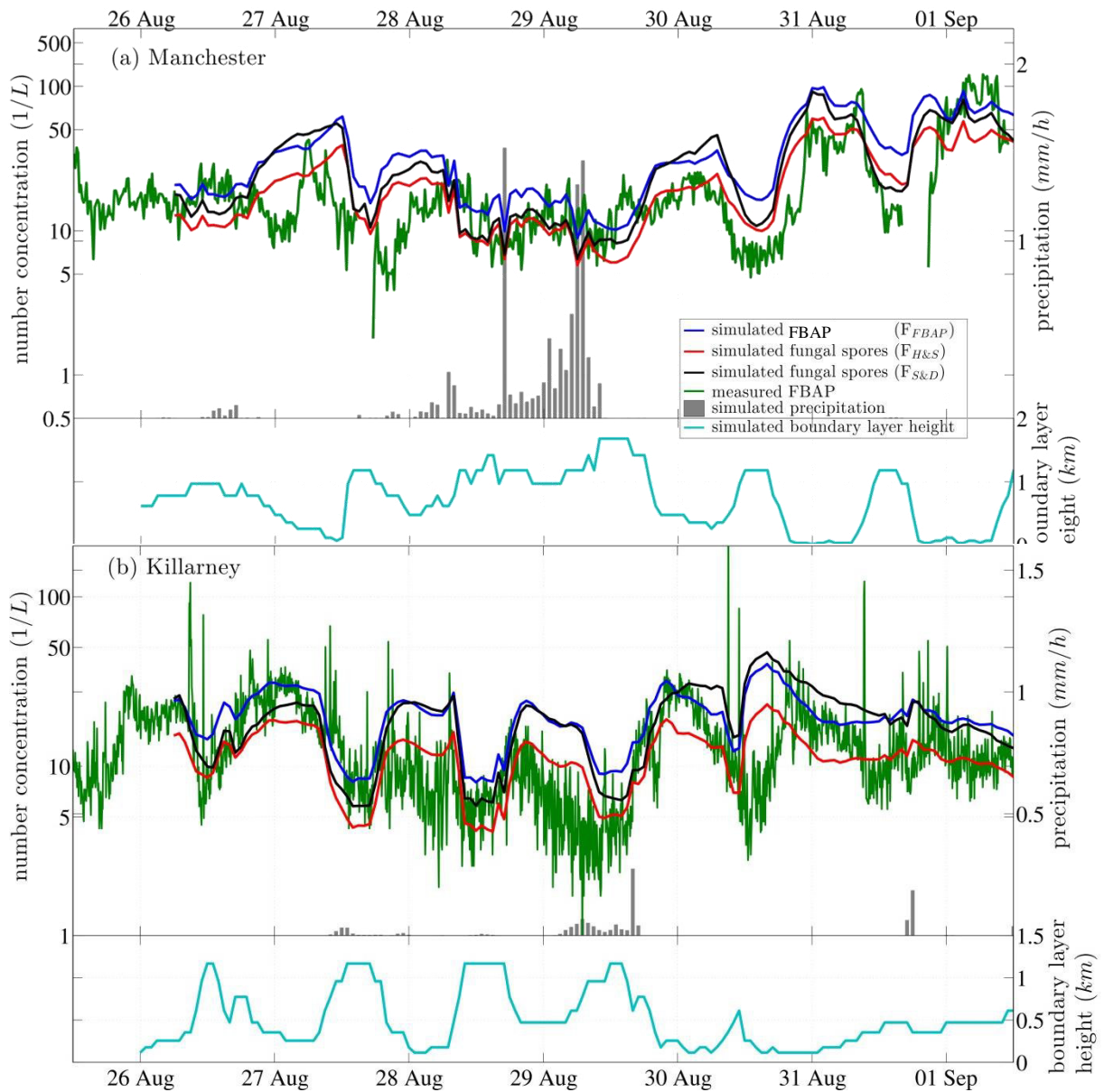
7

8



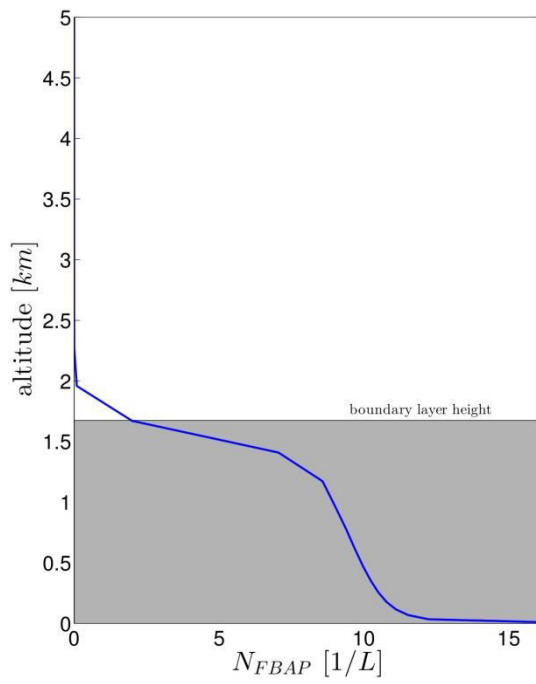
1
 2 Figure 5. Time series of measured FBAP and simulated fungal spore/FBAP number concentrations in 1/L
 3 together with simulated precipitation in mm/h (right axis) and simulated boundary layer height in km (right axis)
 4 during the case study from 26 August 2010 to 01 September 2010 at (a) Karlsruhe, Germany. (b) Hyytiälä,
 5 Finland. Simulations were performed with three different emission parameterizations: $F_{H\&S}$ from Heald and
 6 Spracklen (2009); $F_{S\&D}$ from Sesartic and Dall'afior (2011); F_{FBAP} from this study.

7
 8



1
 2 Figure 6. Time series of measured FBAP and simulated fungal spore number/FBAP concentrations in 1/L
 3 together with simulated precipitation in mm/h (right axis) and simulated boundary layer height in km (right axis)
 4 during the case study from 26 August 2010 to 01 September 2010 at (a) Manchester, UK and (b) Killarney,
 5 Ireland. Simulations were performed with three different emission parameterizations: $F_{H\&S}$ from Heald and
 6 Spracklen (2009); $F_{S\&D}$ from Sesartic and Dallafior (2011); F_{FBAP} from this study.

7

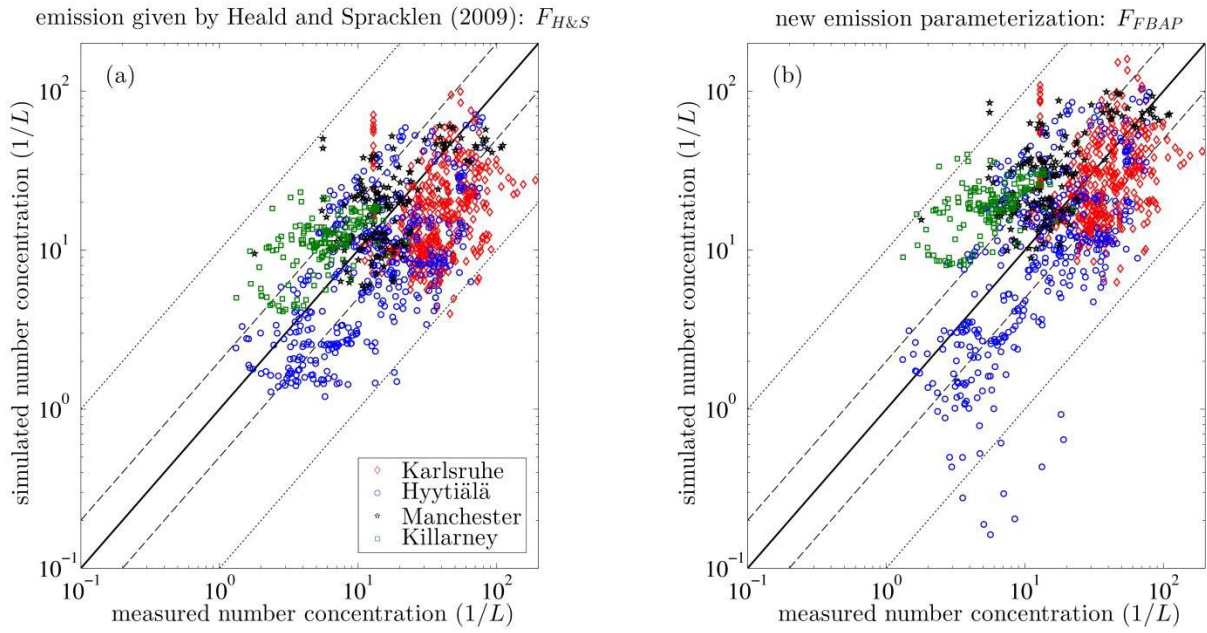


1

2 Figure 7. Exemplary vertical profile of simulated FBAP concentration within and above the planetary boundary
3 layer for Karlsruhe at 28 Aug 2010 14 UTC.

4

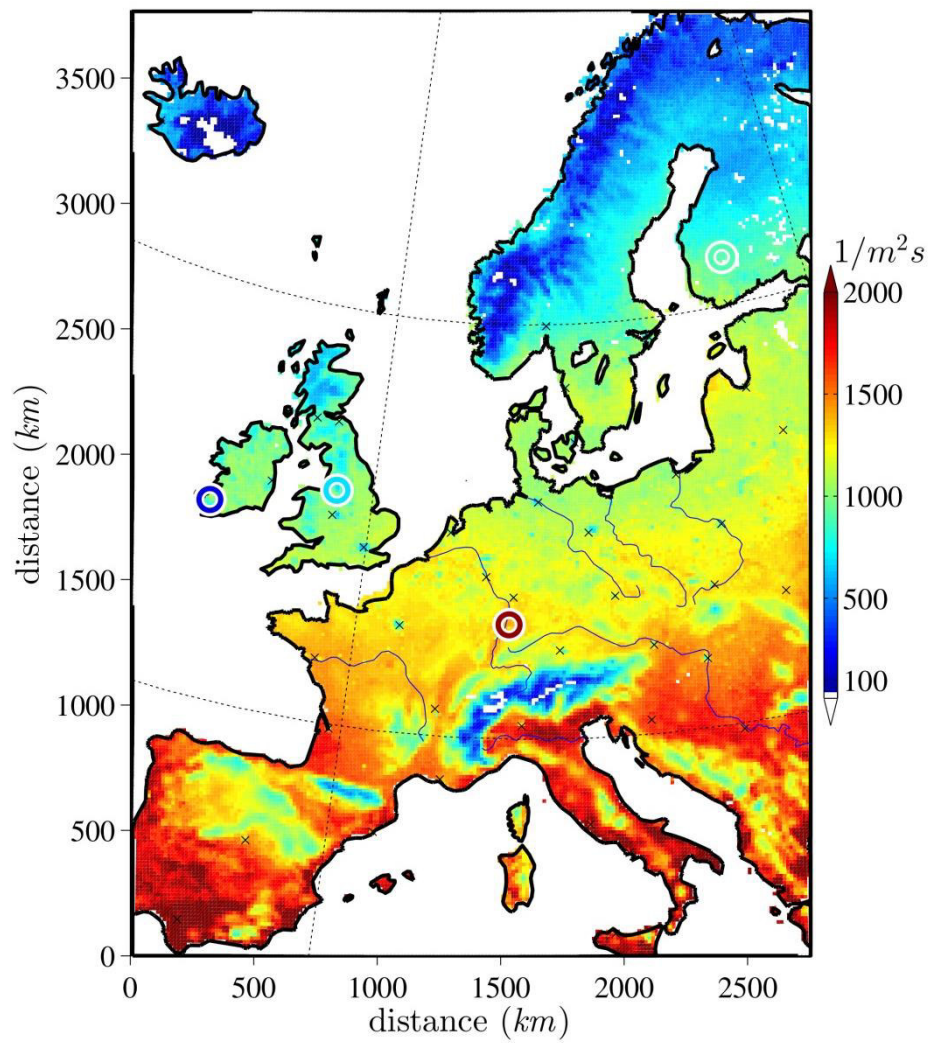
1



2

3 Figure 8. Comparison for all case studies: Measured FBAP number concentrations plotted versus simulated
4 number concentrations of (a) fungal spores based on the Heald and Spracklen (2009) emission flux and (b)
5 FBAP based on the new emission parameterization derived from a multiple linear regression to FBAP
6 concentrations. Solid black lines represent the 1:1-line, dashed lines the 1:2-line and dotted lines the 1:10-line.

7

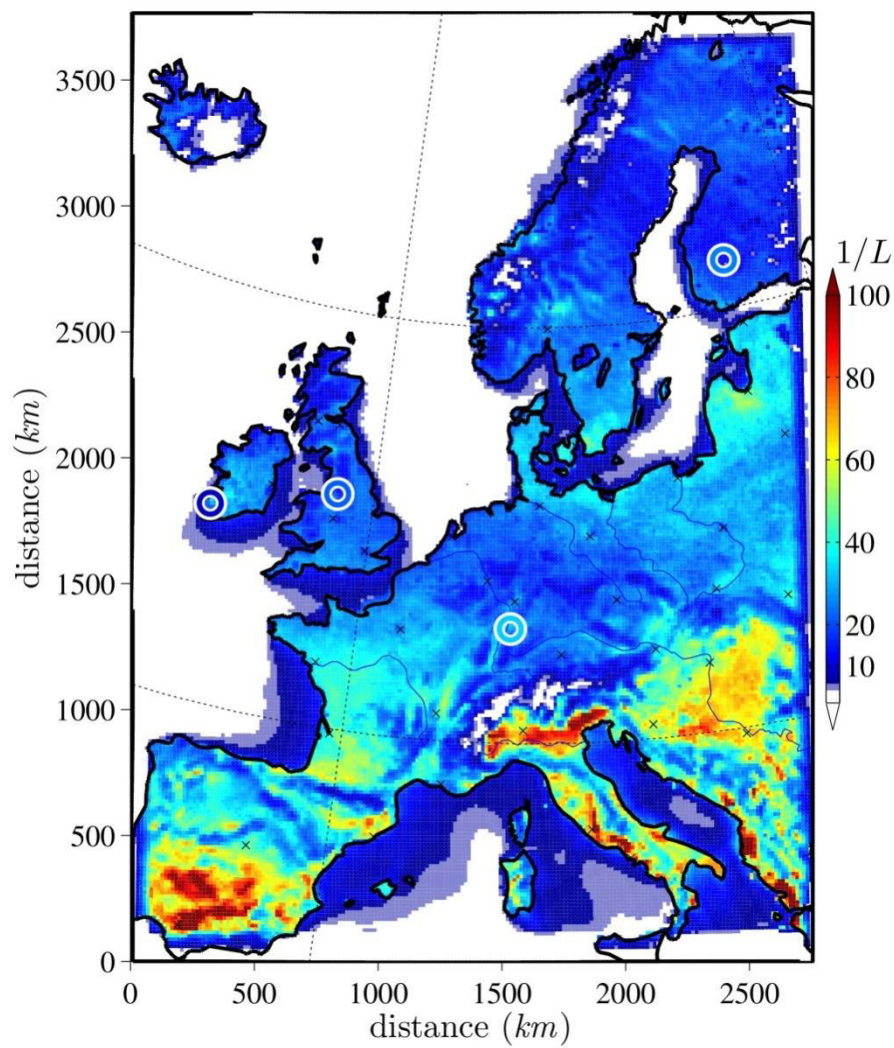


1

2 Figure 9. Average simulated FBAP emission flux (F_{FBAP}) in $m^{-2}s^{-1}$ from 26 August to 01 September 2010,
 3 (excluding a spin-up period of 6 hours). Circles indicate the locations of the different FBAP measurement time
 4 series and the color within the white circles represents the mean emission flux calculated from FBAP
 5 measurements at each location.

6

7

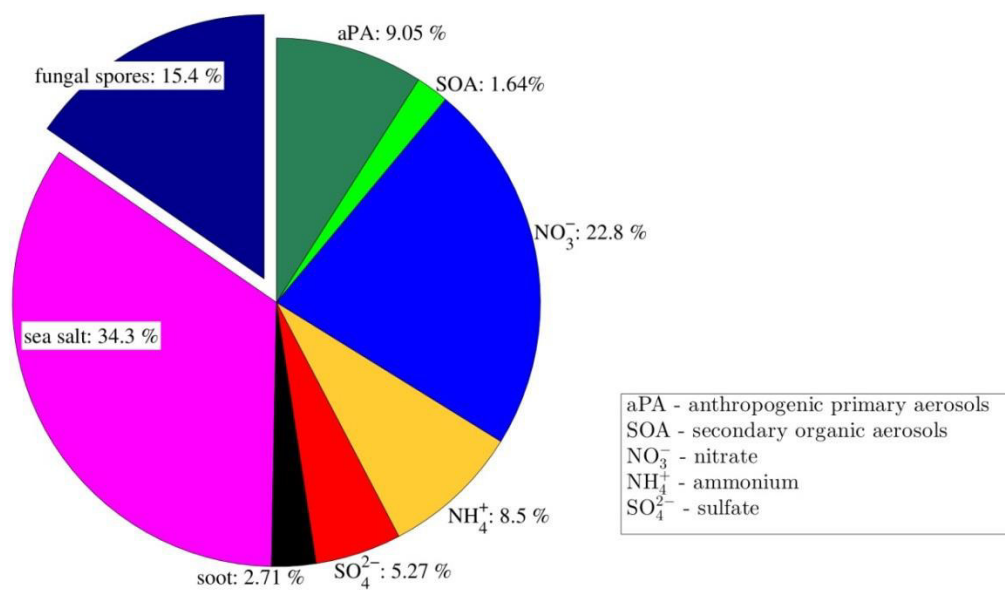


1

2 Figure 10. Horizontally distributed FBAP/fungal spore concentration in $1/L$, emitted by F_{FBAP} , in the lowest
 3 model layer, averaged from 26 August to 01 September 2010 (excluding a spin-up period of 6 hours). Circles
 4 indicate the locations of the different FBAP measurement time series and the color within the white circles
 5 represents the mean FBAP number concentration measured at each location.

6

1



2

3 Figure 11. Near-surface chemical aerosol mass composition simulated by COSMO-ART, horizontally averaged
4 over the land area in the model domain and temporally averaged from 26 August to 01 September 2010
5 (excluding a spin-up period of 6 hours)

6